

Backpressure Flow Control

Prateesh Goyal¹, Preey Shah², Kevin Zhao³, Georgios Nikolaidis⁴,
 Mohammad Alizadeh¹, Thomas E. Anderson³

¹MIT CSAIL, ²IIT Bombay, ³University of Washington, ⁴Intel, Barefoot Switch Division

Abstract

Effective congestion control for data center networks is becoming increasingly challenging with a growing amount of latency-sensitive traffic, much fatter links, and extremely bursty traffic. Widely deployed algorithms, such as DCTCP and DCQCN, are still far from optimal in many plausible scenarios, particularly for tail latency. Many operators compensate by running their networks at low average utilization, dramatically increasing costs.

In this paper, we argue that we have reached the practical limits of end-to-end congestion control. Instead, we propose, implement, and evaluate a new congestion control architecture called *Backpressure Flow Control* (BFC). BFC provides per-hop per-flow flow control, but with bounded state, constant-time switch operations, and careful use of buffers. We demonstrate BFC’s feasibility by implementing it on a state-of-the-art P4-based programmable hardware switch. In simulation, we show that BFC achieves near optimal throughput and tail latency behavior even under challenging conditions such as high network load and incast cross traffic. Compared to existing end-to-end schemes, BFC achieves 2.3 - 60 \times lower tail latency for short flows and 1.6 - 5 \times better average completion time for long flows.

1 INTRODUCTION

Single and multi-tenant data centers have become one of the largest and fastest growing segments of the computer industry. Data centers are increasingly dominating the market for all types of high-end computing, including enterprise services, parallel computing, large scale data analysis, fault-tolerant middleboxes, and global distributed applications [8, 24, 41]. These workloads place enormous pressure on the data center network to deliver, at low cost, ever faster throughput with low tail latency even for highly bursty traffic [21, 56].

Although details vary, almost all data center networks today use a combination of endpoint congestion control, FIFO queues at switches, and end-to-end feedback of congestion signals like delay or explicit switch state to the endpoint control loop.¹ As link speeds continue to increase, however, the design of the control loop becomes more difficult. First, more traffic fits within a single round trip, making it more difficult to use feedback effectively. Second, traffic becomes increasingly bursty, so that network load is not a stable property except over very short time scales. And third, switch buffer capacity is not keeping up with increasing link speeds, making it even more challenging to handle traffic bursts. Most network operators run their networks

at very low average load, throttle long flows at far below network capacity, and even then see significant congestion loss.

Instead, we propose a different approach. The key challenge for data center networks, in our view, is to efficiently allocate buffer space at congested network switches. This becomes easier and simpler when control actions are taken per flow and per hop, rather than end-to-end. Despite its advantages, per-hop per-flow flow control appears to require per-flow state at each switch, even for quiescent flows [9, 36], something that is not practical at data center scale.

Our primary contribution is to show that per-hop per-flow flow control can be *approximated* with a modest and limited amount of switch state, using only simple constant-time switch operations on a modern programmable switch. Unlike receiver-driven congestion control like NDP [27] and Homa [44], our approach assumes congestion can occur anywhere (not just the last hop) and generalizes to asymmetric and oversubscribed topologies. Unlike prior work in per-hop flow control, our approach is not completely loss-free, so we assume an end-to-end recovery system such as Go-back-N, SACK [22], or IRN [43].

We have implemented our approach, *Backpressure Flow Control* (BFC), on a state-of-the-art P4-based programmable switch ASIC supporting 12.8 Tbps of switching capacity. To preserve anonymity we refer to this as SwitchX. Our implementation uses less than 10% of the dedicated stateful memory on SwitchX. All per-packet operations are implemented entirely in the dataplane; BFC runs at full switch capacity.

To evaluate performance, we run large-scale ns-3 [3] simulations using synthetic traces drawn to be consistent with measured workloads from Google and Facebook data centers [44] on an oversubscribed multi-level Clos network topology. We show that BFC, unlike DCTCP, DCQCN, and HPCC, achieves close to optimal throughput and tail latency performance for short, medium, and long flows, even when the network is heavily loaded or disrupted by incast traffic. Compared to existing schemes, BFC achieves 2.3 - 60 \times better tail flow completion times (FCTs) for short flows, and 1.6 - 5 \times better average performance for long flows. Our simulation code will be made public and is available to the reviewers on request.

Our specific contributions are:

- A discussion of the fundamental limits of end-to-end congestion control for high bandwidth data center networks.
- A practical protocol for per-hop per-flow flow control, called BFC, that uses a small, constant amount of state to achieve near-optimal tail-latency performance for typical data center workloads.

¹We refer to schemes that rely on feedback signals delayed by an entire round-trip time as *end-to-end* schemes, to contrast them with hop-by-hop mechanisms.

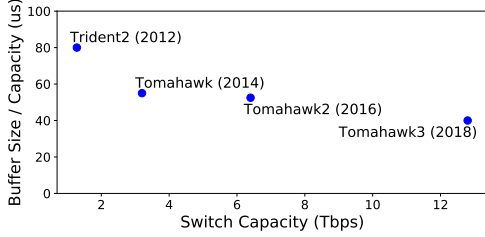


Figure 1: Hardware trends for top-of-the-line data center switches from Broadcom. Switch capacity and link speed have been growing rapidly, but buffer size is not keeping up with increases in switch capacity.

- An implementation and proof-of-concept evaluation of BFC on a commodity switch. To our knowledge, this is the first implementation of a per-hop per-flow flow control scheme for a multi-Tbps switch.

2 MOTIVATION

Over the last decade, researchers and data center operators have proposed a variety of congestion control algorithms for data centers, including DCTCP [6], Timely [42], Swift [35], DCQCN [59], and HPCC [38]. The primary goals of these protocols are to achieve high throughput, low tail packet delay, and high resilience to bursts and incast traffic patterns. Operationally, these protocols rely on *end-to-end* feedback loops, with senders adjusting their rates based on congestion feedback signals echoed by the receivers. Irrespective of the type of signal (e.g., ECN marks, multi-bit INT information [31, 38], delay), the feedback delay for these schemes is a network round-trip time (RTT). This delay has an important role in the performance of end-to-end schemes. In particular, senders require at least one RTT to obtain feedback, and therefore face a hard tradeoff in deciding the starting rate of a flow. They can either start at a high rate and risk causing congestion, or start at a low rate and risk under-utilizing the network. Moreover, even after receiving feedback, senders can struggle to determine the right rate if the state of the network (e.g., link utilization and queuing delay) changes quickly compared to the RTT.

We argue that three trends are making these problems worse over time, and will make it increasingly difficult to achieve good performance with end-to-end protocols.

Trend 1: Rapidly increasing link speed. Fig. 1 shows the switch capacity of top-of-the-line data center switches manufactured by Broadcom [17, 45]. Switch capacity and link speeds have increased by a factor of 10 over the past six years with no signs of stopping.

Trend 2: Most flows are short. Fig. 2 shows the byte-weighted cumulative distribution of flow sizes for three industry data center workloads [44]: (1) All applications in a Google data center, (2) Hadoop cluster in a Facebook center, and (3) a WebSearch workload. Each point is the fraction of all bytes sent that belong to flows smaller than a threshold for that workload. For example, for the Google workload, flows that are shorter than 100 KB represent nearly half of all bytes. Flows that are smaller than the bandwidth-delay-product (BDP) can ideally

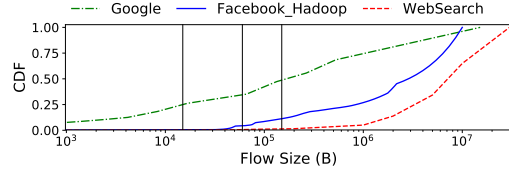


Figure 2: Cumulative bytes contributed by different flow sizes for three different industry workloads. The three vertical lines show the BDP for a 10 Gbps, 40 Gbps, and 100 Gbps network, assuming a 12 μ s RTT.

complete within one RTT, if the sender begins transmitting at line rate. As link speed increases, such flows represent a growing fraction of traffic. For example, most Facebook Hadoop traffic is likely to fit within one round trip within the next decade. While some have argued that data center flows are increasing in size [5], the trend is arguably in the opposite direction with the growing use of RDMA for fine-grained remote memory access.

Trend 3: Buffer size is not scaling with switch capacity.

Fig. 1 shows that the switch buffer size relative to its capacity has decreased by a factor of 2 (from 80 μ s to 40 μ s) over the past six years. With smaller buffers relative to link speed, buffers now fill up more quickly, making it more difficult for end-to-end congestion control to manage those buffers. The limiting factor is chip area — buffers and switching capacity compete for room on the same die, and better management of switch buffers would allow for higher capacity switches.

2.1 Limits of End-to-End Congestion Control

This combination — very fast links, short flows, and inadequate buffers — create the perfect storm for end-to-end congestion control protocols. Flows that complete within one or a few RTTs (which constitute an increasingly larger fraction of traffic) either receive no feedback, or last for so few feedback cycles that they cannot find the correct rate [30]. For longer flows, the rapid arrival and departure of cross-traffic creates significant fluctuations in available bandwidth at RTT timescales, making it difficult to find the correct rate. The result is loss of throughput and large queue buildup. Insufficient switch buffering further exacerbates these problems, leading to packet drops or link-level pause events (PFC [54]) that spread congestion upstream.

Fig. 3 shows the variance in the fair share rate for a long-lived flow competing on a single link with flows derived from the Facebook workload. We repeat the experiment at 10, 40, and 100 Gbps, and set the average load of the cross-traffic flows to be 60% of the link capacity in each case. As link speed increases, cross-traffic flows arrive and finish more quickly, and the fair-share rate at the bottleneck link changes more rapidly. We also simulate two state-of-the-art congestion control protocols, DCQCN and HPCC, for this scenario. Especially at higher link speeds, neither comes close to delivering the available bandwidth to the long flow or maintaining small queues for short flows.

2.2 Existing Solutions are Insufficient

There are several existing solutions that go beyond end-to-end congestion control. We briefly discuss the most prominent of

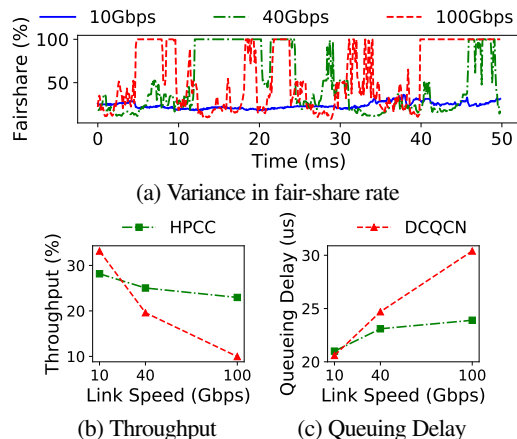


Figure 3: Variance in fair share rate, average throughput of a long-lived flow, and 99th percentile queuing delay experienced by single-packet flows. The available capacity for the long-lived flow in these experiments is 40%.

these approaches and why they are insufficient to deal with the challenges described above.

Priority flow control (PFC). One approach to handling increased buffer occupancy would be to use PFC, a hop-by-hop flow control mechanism.² With PFC, if the packets from a particular input port start building up at a congested switch (past a configurable threshold), the switch sends a “pause” frame upstream, stopping that input from sending more traffic until the switch has a chance to drain stored packets. This prevents switch buffers from being overrun. Unfortunately, PFC has a side effect: head-of-line (HoL) blocking [59]. For example, incast traffic to a single server can cause PFC pause frames to be sent one hop upstream towards the source of the traffic. This stops *all* the traffic traversing the paused link, even those flows that are destined to other uncongested egress ports. These flows will be delayed until the packets at the congested port can be drained. Worse, as packets queue up behind a PFC, additional PFC pause frames can be triggered at upstream hops, widening the scope of HoL-blocking.

Switch scheduling. Several efforts use switch scheduling to overcome the negative side-effects of elephant flows on the latency of short flows. These proposals range from approximations of fair queuing (e.g., Stochastic Fair Queuing [40], Approximate Fair Queuing [48]) to scheduling policies that prioritize short flows (e.g., pFabric [7], QJump [25], Homa [44]). While such scheduling policies can improve flow completion times, they cannot prevent packet drops or HoL-blocking due to PFC pause frames, given today’s buffer-constrained switches (§6.2.2). The problem is that scheduling by itself does nothing to reduce buffer occupancy. As link speeds increase, the fair share rate becomes more variable, and performance will suffer with end-to-end congestion control regardless of the scheduling policy.

Receiver-based congestion control. Because sender-based congestion control systems generally perform poorly on incast

workloads, some researchers have proposed shifting to a scheme where the receiver prevents congestion by explicitly allocating credits to senders for sending traffic. Three examples are NDP [27], pHost [23] and Homa [44]. However, these schemes can only address congestion that occurs at the last hop, where the receiver has complete visibility. In practice, over-subscription is common, and measurements of production data center networks suggest that congestion can occur throughout the network [49]. Other proposals suggest collecting credits from all switches in the path before sending [19, 55, 57]; at high link speeds, there is low auto-correlation in the fair share rate over short time scales (Fig. 3), making that problematic.

2.3 Revisiting Per-hop, Per-Flow Flow Control

Our approach is inspired by work in the early 90s on hop-by-hop credit-based flow control for managing gigabit ATM networks [9, 36]. Credit-based flow control was also introduced by multiprocessor hardware designs of the same era [16, 33, 37]. In these systems, each switch methodically tracks its buffer space, granting permission to send at an upstream switch if and only if there is room in its buffer. In ATM, packets of different flows are buffered in separate queues and are scheduled according to the flows’ service requirements. The result is a network that has no congestion loss by design.

An ideal realization of such a per-hop, per-flow flow control scheme has several desirable properties:

(1) Fast reaction: When a flow starts experiencing congestion at a switch, the upstream switch can reduce its rate within a 1-hop RTT, instead of the end-to-end RTT that it takes for standard congestion control schemes. Likewise, when capacity becomes available at a switch for a particular flow, the upstream switch can send it packets within a 1-hop RTT (provided the upstream switch has packets from that flow). Assuming a hardware implementation, the 1-hop RTT consists of the propagation latency and the switch pipeline latency — typically 1-2 μ s.³ This is substantially smaller than the typical end-to-end RTT in data centers (e.g., 10-20 μ s), which in addition to multiple switch hops includes the latency at the endpoints.

(2) Buffer pooling: During traffic bursts, a per-hop per-flow flow control mechanism throttles traffic upstream from the bottleneck. This enables the bottleneck switch to tap into the buffers of its upstream neighbors, thereby significantly increasing the ability of the network to absorb bursts.

(3) No HoL-blocking: Unlike PFC, there is no HoL-blocking or congestion spreading with per-hop per-flow flow control, because switches isolate flows in different queues and perform flow control for each of them separately.

(4) Simple control actions: Flow control decisions in a per-hop per-flow flow control system are simpler to design and reason about than end-to-end congestion control algorithms because: (i) whether to send or pause a flow at a switch depends only on feedback from the immediate next-hop switch (as opposed to

²For simplicity, we focus on the case where there is congestion among the traffic at a particular priority level.

³For example, a 100 m cable has a propagation latency of 500 ns, and a typical data center switch has a pipeline latency around 500 ns [12, 17].

Scheme	Throughput (%)	99% Queuing Delay (μ s)
BFC	37.3	1.2
HPCC	22.9	23.9
DCQCN	10.0	30.4
HPCC + SFQ	21.9	15.9

Table 1: For a shared link with a long flow, BFC achieves close to ideal throughput (40%) for the long flow, with lower tail queuing delay. Same setup as Fig. 3 on 100 Gbps links.

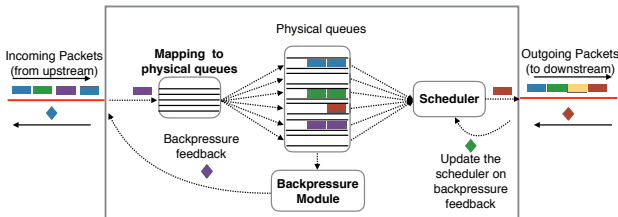


Figure 4: Logical switch components in per-hop, per-flow flow control.

multiple potential points of congestion with end-to-end schemes), (ii) concerns like fairness are dealt with trivially by scheduling flows at each switch, and therefore flow control can focus exclusively on the simpler task of managing buffer occupancy and ensuring high utilization.

Despite these compelling properties, per-hop per-flow flow control schemes have not been widely deployed, in part because of their high implementation complexity and resource requirements. As we detail in the next section, traditional ATM schemes require per-connection state and large buffers, and are not feasible to implement in today’s data center switches. The principal contribution of our work is a practical design called Backpressure Flow Control (BFC). BFC differs from ATM approaches in several ways: it uses on/off pause frames rather than credits; it operates with a relatively small number (e.g., 10s) of physical queues per port; it carefully manages buffer space to work within the bounds of current hardware; and, critically, *it does not require per-connection state*. BFC can be implemented using only constant-time switch operations on a modern programmable switch. BFC is not perfectly lossless, but it makes losses extremely rare.

As an example of BFC’s performance benefits, we repeat the experiment in Fig. 3 with a single long-lived flow competing against variable cross-traffic with 60% average load at 100 Gbps link speed. Additionally, we include HPCC + SFQ (i.e., HPCC with stochastic fair queuing at the switches) in the results. Table 1 shows that BFC is able to achieve close to the maximum possible throughput for the long-lived flow (40%), while reducing 99th percentile queuing delay compared to the other schemes.

3 DESIGN

Our goal is to design a practical system for per-hop, per-flow flow control for data center networks. We first describe the constraints on our design (§3.1). We then sketch a plausible strawman proposal that surprisingly turns out to not work well at all (§3.2), and we use that as motivation for our design (§3.3).

3.1 Design Constraints

Fig. 4 shows the basic components of a per-hop, per-flow flow control scheme (per port). (1) *Mapping to physical queues*: When a packet arrives at the switch, the switch routes the packet to an egress port and maps it to a FIFO queue at that port. This assignment of flows to queues must be consistent, that is, respect packet ordering. (2) *Backpressure module*: Based on queue occupancy, the switch generates backpressure feedback for some flows and sends it upstream. (3) *Scheduler*: The scheduler at each egress port forwards packets from queues while respecting backpressure feedback from the downstream switch.

ATM per-hop per-flow flow control systems [9, 36] roughly followed this architecture, but they would be impractical for modern data centers. First, they assumed per-flow queues and per-flow state, but modern switches have a limited number of queues per egress port [14, 48] and modest amounts of table memory [15, 20]. In particular, it is not possible to maintain switch state for all live connections. Second, earlier schemes did not attempt to minimize buffer occupancy. Instead, they sent backpressure feedback only when the switch was about to run out of buffers. On a buffer-constrained switch, this can result in buffer exhaustion — buffers held by straggler flows can prevent other flows from using those buffers at a later time.

Hardware assumptions. Modern data center switches have made strides towards greater flexibility [10, 51], but they are not infinitely malleable and have real resource constraints. We make the following assumptions based on the capabilities of SwitchX.

1. We assume the switch is programmable and supports stateful operations for hundreds of thousands of entries. SwitchX can maintain millions of register entries; the switch supports simple constant-time per-packet operations to update the state at line rate [50].
2. The switch has a limited number of FIFO queues per egress port, meaning that flows must be multiplexed onto queues. SwitchX has 32 queues per 100G port and 128 per 400G port. The assignment of flows to queues is programmable. The scheduler can use deficit round-robin or priorities among queues, but packets within a queue are forwarded in FIFO order.
3. Each queue can be independently paused and resumed without slowing down forwarding from other queues. However, when we pause a queue, that pauses *all* of the flows assigned to that queue.
4. The switch can pause/resume each queue separately from the (programmable) dataplane. Earlier switches can pause/resume individual queues, but only from the control plane. This is likely too slow for effective hop-by-hop control. In contrast, SwitchX allows for fast, programmable pause/resume scheduling from the dataplane itself.

3.2 A Strawman Proposal

We originally thought stochastic fair queueing [40] with per-queue backpressure would meet our goals. Use a hash function on the flow header to consistently assign the packets of each flow to

a randomly-chosen FIFO queue at its egress port. For simplicity, use the same hash function at each switch. Pause a queue whenever its buffer exceeds the 1-hop bandwidth-delay product (BDP).

This strawman needs only a small amount of state for generating the backpressure feedback and no state for queue assignment. It seems like we should be done, and this paper could be short. However, the strawman proposal does not work well. With even a modest number of active flows, there is a significant chance that any specific flow will land in an already-occupied FIFO queue. These collisions hurt latency for two reasons: (1) The packets for the flow will be delayed behind unrelated packets from other flows; for example, a short flow may land behind a long flow. (2) Queue sharing can cause HoL-blocking. If a particular flow is paused (because it is congested downstream), all flows sharing the same queue will be delayed. Furthermore, these delays can cause cascading pauses further upstream.

These problems occur with stochastic fair queueing even when we have enough physical resources to give each active flow its own dedicated FIFO queue. We define an *active* flow as one with queued packets at the switch. The birthday paradox [1] implies stochastic collisions between active flows will be frequent. For example, when five active flows are assigned to 32 FIFO queues, the chance that at least two flows will be randomly assigned to the same queue is 28%. Further, a flow going through multiple switches can experience such collisions at each of its hops. Since data center operators care about tail latency (95th or 99th percentile), avoiding collisions, even to a small percentage of flows, is important. Moreover, collisions slow down flows and increase the number of active flows, driving up the collisions further.

To prevent collisions from affecting tail latency performance, the strawman requires significantly more queues than active flows. For example, at an egress port with n active flows, to achieve fewer than 1% collisions, we would need roughly $100n$ queues.

3.3 Backpressure Flow Control (BFC)

Our design achieves the following properties:

Minimal HoL-blocking: We assign flows to queues dynamically. As long as the number of active flows at an egress is less than the number of queues, (with high probability) no two flows share a queue and there is no HoL-blocking. When a new flow arrives at the switch, it is assigned to an empty queue if one is available, sharing queues only if all are in use.

Low buffering and high utilization: BFC pauses a flow at the upstream when the queue occupancy exceeds a small threshold. BFC’s pause threshold is set aggressively to reduce buffering. With a blanket pause system like PFC, pausing aggressively hurts link utilization, but BFC only pauses those flows causing congestion (except when collisions occur). The remaining flows at the upstream can continue transmitting, avoiding under-utilization. BFC’s pausing mechanism is compatible with any scheduling policy (e.g., priorities, hierarchical fair queuing, etc.). For concreteness, we constrain our discussion to fair queuing.

Hardware Feasibility: BFC does not require per-flow state, and instead uses an amount of memory proportional to the number

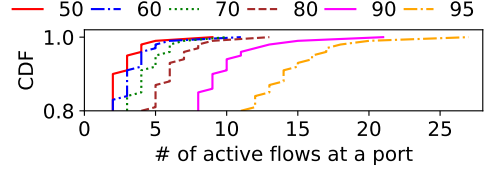


Figure 5: Number of active flows versus aggregate load on a single 100 Gbps link. Flow sizes are derived from the Facebook distribution, with Poisson flow arrivals.

of physical queues in the switch. To allow efficient lookup of the state associated with a flow, the state is stored in a flow table, an array indexed using a hash of the flow identifier. The size of this array is set in proportion to the number of physical queues. In our SwitchX implementation, it consumes less than 10% of the dedicated stateful memory. Critically, the mechanism for generating backpressure and reacting to it is simple and the associated operations can be implemented entirely in the dataplane at line rate.

Generality: BFC does not make assumptions about the network topology or where congestion occurs in the network. By contrast, schemes like NDP [27], pHost [23] and Homa [44] assume sufficient core network bandwidth and congestion is only at the last hop. Furthermore, unlike pFabric [7] and Homa [44], BFC does not assume knowledge about flow sizes or deadlines. Such information can be incorporated into BFC’s design to improve small flow performance (App. E.2), at a cost in deployability.

Idempotent state: Because fiber packets can be corrupted in flight [60], BFC ensures that pause and resume state is maintained idempotently, in a manner resilient to packet loss.

3.3.1 Assigning flows to queues

To minimize sharing of queues and HoL-blocking, we dynamically assign flows to empty queues. As long as the flow is active (has packets queued at the switch), subsequent packets for that flow will be placed into the same FIFO queue. Each flow has a unique 5-tuple of the source and destination addresses, port numbers, and protocol; we call this the flow identifier (FID). BFC uses the hash of the FID to track a flow’s queue assignment. To simplify locating an empty queue, BFC maintains a bit map of empty queues. When the last packet in a queue is scheduled, BFC resets the corresponding bit for that queue.

With dynamic queue assignment, a flow can be assigned to different queues at different switches. To pause a flow, BFC pauses the queue the flow came from at the upstream switch (called the upstream queue). The pause applies to all flows sharing the same upstream queue with the paused flow. We describe the pause mechanism in detail in §3.3.2. The packet scheduler uses deficit round robin to implement fair queueing, among the queues that are not paused.

Since there is a limited number of queues, it is possible that all queues have been allocated when a new flow arrives, at which point HoL-blocking is unavoidable. For hardware simplicity, we assign the flow to a random queue in this case. Packets assigned to the same queue are scheduled in FIFO order.

BFC incurs collisions only when the number of *active flows*

i.e., flows with packets in the switch, exceeds the number of queues at an egress port. (Note that the total number of connections (including idle flows) traversing the port may be much higher.) A fundamental result of queueing theory is that the number of active flows at a fair queued switch is surprisingly small, even at high load [32, 34]. In particular, for an M/G/1-PS (Processor Sharing) queue with Poisson flow arrivals operating at average load $\rho < 1$, the number of active flows has a geometric distribution with mean $\frac{\rho}{1-\rho}$, independent of the link speed or the flow size distribution. Therefore, even at load $\rho = 0.95$, the expected number of active flows is only 19. To illustrate this result in practice, Fig. 5 shows the cumulative distribution of the number of active flows for BFC at an egress port, with a workload using the Facebook flow size distribution and Poisson flow arrivals. We see that at 95% load, the number of active flows is at most ~ 30 . The high-level intuition is that in a fair-queueing system, each flow gets equal service, and therefore a large, congested flow cannot disproportionately slow down other flows. By contrast, in a FIFO system, a single large flow can prevent service for many small flows, thereby sharply increasing the number of active flows.

Of course, the number of active flows can still exceed the number of queues in settings with bursty flow arrivals (e.g., incast). BFC incurs some HoL-blocking in such scenarios, but it still outperforms prior approaches even in these extreme cases (see §6.2.3). In particular, in case of an incast, BFC can leverage the large number of upstream queues feeding traffic to a switch to limit congestion spreading. The observation is that, when flows involved in an incast are spread among multiple upstream ports, BFC can assign these flows to separate queues at those ports, as long as the total number of flows does not exceed the total number of queues across *all* of the upstream ports. In such cases, BFC will not incur HoL-blocking at the upstream switches. As the size of the network increases and the fan-in to each switch gets larger, there will be even more queues at the upstream switches to absorb an incast, further reducing congestion spreading.

Mechanism: To keep track of queue assignment, BFC maintains an array indexed by the egress port of a flow and the hash of the FID. All flows that map to the same index are assigned to the same queue. We maintain the following state per entry: the physical queue assignment (`qAssignment`), and the number of packets in the queue from the flows mapped to this entry (`size`). The pseudocode is as follows (we defer switch-specific implementation issues to §6.1):

```
On Enqueue(packet):
    key = <packet.egressPort, hash(packet.FID)>
    if flowTable[key].size == 0:
        reassignQueue = True:
    flowTable[key].size += 1
    if reassignQueue:
        if empty q available at packet.egressPort:
            qAssignment = emptyQ
        else:
            qAssignment = randomQ
    flowTable[key].qAssignment = qAssignment
    packet.qAssignment = flowTable[key].qAssignment
```

```
On Dequeue(packet):
    key = <packet.egressPort, hash(packet.FID)>
    flowTable[key].size -= 1
```

In the flow table, if two flows map to the same index they will use the same queue (collision). Since flows going through different egress ports cannot use the same queue, the index also includes the egress port. Index collisions in the flow table can hurt performance. These collisions decrease with the size of the table, but the flow table cannot be arbitrarily large as the switch has a limited stateful memory. In our design, we set the size of the flow table to $100 \times$ the number of queues in the switch. This ensures that if the number of flows at an egress port is less than the number of queues, then the probability of index collisions is less than 1%. If the number of flows exceeds the number of queues, then the index collisions do not matter as there will be collisions in the physical queues regardless. SwitchX has 4096 queues in aggregate, and hence the size of the flow table is 409,600 entries, which is less than 10% of the switch’s dedicated stateful memory.

While using an array is not memory efficient, accessing state involves simple operations. Existing solutions for maintaining flow state either involve slower control plane operations, or are more complex [11, 46]. In the future, if the number of queues increases substantially, we can use these solutions for the flow table, however at the moment, the additional complexity is unnecessary.

3.3.2 Backpressure mechanism

BFC pauses a flow if the occupancy of the queue assigned to that flow exceeds the pause threshold Th . To pause/resume a flow, the switch could signal the flow ID to the upstream switch, which can then pause/resume the queue associated with the flow. While this solution is possible in principle, it is difficult to implement on today’s programmable switches. The challenge is that, on receiving a pause, the upstream switch needs to perform a reverse lookup to find the queue assigned to the flow and some additional bookkeeping to deal with cases when a queue has packets from multiple flows (some of which might be paused and some not).

We take a different approach. Switches directly signal to the upstream device to pause/resume a specific queue. Each upstream switch/source NIC inserts its local queue number in a special header field called `upstreamQ`. The downstream switch stores this information in the flow table and uses it to pause the queue at the upstream.

Mechanism: Recall that, in general, multiple flows can share a queue even if that is the rare case. This has two implications. First, we track the queue length (and not just the `flowTable.size`) and use that to determine if the flow’s upstream queue should be paused. Second, each upstream queue can, in general, feed data into multiple queues at multiple egresses. We pause an upstream queue if *any* of its flows are assigned a congested queue, and we resume when *none* of its flows have packets at a congested queue (as measured at the time the packet arrived at the switch).

We monitor this using a Pause Counter, an array indexed by the ingress port and the `upstreamQ` of a packet. The upstream queue is paused if and only if its Pause Counter at the downstream switch is non-zero. On enqueue of a packet, if its flow is assigned

a queue that exceeds the pause threshold, we increment the pause counter at that index by 1. When this packet (the one that exceeded Th) leaves the switch we decrement the counter by 1. Regardless of the number of flows assigned to the `upstreamQ`, it will be resumed only once all of its packets that exceeded the pause threshold (when the packet arrived) have left the switch.

```
On Enqueue(packet):
    key = <packet.ingressPort, packet.upstreamQ>
    if packet.qAssignment.qLength > Th:
        if pauseCounter[key] == 0:
            // Pause the queue at upstream
            sendPause(key)
        pauseCounter[key] += 1
        packet.metadata.counterIncr = True

On Dequeue(packet):
    key = <packet.ingressPort, packet.upstreamQ>
    if packet.metadata.counterIncr == True:
        pauseCounter[key] -= 1
        if pauseCounter[key] == 0:
            // Resume the queue at upstream
            sendResume(key)
```

To minimize bandwidth consumed in sending pause/resumes, we only send a pause packet when the pause counter for an index goes from 0 to 1, and a resume packet when it goes from 1 to 0. For reliability against pause/resume packets being dropped, we also periodically send a bitmap of the queues that should be paused at the upstream (using the pause counter). Additionally, the switch uses a high priority queue for processing the pause/resume packets. This reduces the number of queues available for dynamic queue assignment by 1, but it eliminates performance degradation due to delayed pause/resume packets.

The memory required for the pause counter is small compared to the flow table. For example, if each upstream switch has 128 queues per egress port, then for a 32-port downstream switch, the pause counter is 4096 entries.

Pause threshold. BFC treats any queue buildup as a sign of congestion. BFC sets the pause threshold Th to 1-Hop BDP at the queue drain rate. Let N_{active} be the number of *active queues* at an egress, i.e. queues with data to transmit that are not paused, $HRTT$ be the 1-Hop RTT to the upstream, and μ be the port capacity. Assuming fair queuing as the scheduling policy, the average drain rate for a queue at the egress is μ/N_{active} . The pause threshold Th is thus given by $(HRTT) \cdot (\mu/N_{active})$. When the number of active queues increases, Th decreases. In asymmetric topologies, egress ports can have different link speeds; as a result, we calculate a different pause threshold for every egress based on its speed. Similarly, ingress ports can have different 1-Hop RTTs. Since a queue can have packets from different ingresses, we use the max of $HRTT$ across all the ingresses to calculate Th . We use a pre-configured match-action table indexed with N_{active} and μ to compute Th .

BFC does not guarantee that a flow will never run out of packets due to pausing. First, a flow can be paused unnecessarily if it is sharing its upstream queue with other paused flows. Second, a switch only resumes an upstream queue once all its packets (that exceeded the pause threshold when they arrived)

have left the downstream switch. Since the resume takes an $HRTT$ to take effect, a flow can run out of packets at the downstream switch for an $HRTT$, potentially hurting utilization. However, this scenario is unlikely — a pause only occurs when a queue builds up, typically because multiple flows are competing for the same egress port. In this case, the other flows at the egress will have packets to occupy the link, preventing under-utilization.

We might reduce the (small) chance of under-utilization by resuming the upstream queue earlier, for example, when a flow’s queue at the downstream drops below Th , or more precisely, when *every* queue (with a flow from the same upstream queue) drops below Th . Achieving this would require extra bookkeeping, complicating the design.

Increasing the pause threshold would reduce the number of pause/resumes generated, but only at the expense of increased buffering (Fig. 7). In App. A, we analyze the impact of Th on under-utilization and peak buffer occupancy in a simple model, and we show that a flow runs out of packets at most 20% of the time when Th is set to 1-hop BDP. Our evaluation results show that BFC achieves much better throughput than this worst case in practice (Table 1, §6).

Sticky queue assignment: Using `upstreamQ` for pausing flows poses a challenge. Since a switch does not know the current queue assignment of a flow at the upstream, it uses the `upstreamQ` conveyed by the last packet of the flow to pause a queue. However, if a flow runs out of packets at the upstream switch (e.g., because it was bottlenecked at the downstream switch but not the upstream), then its queue assignment may change for subsequent packets, causing it to temporarily evade the pause signal sent by the downstream switch. Such a flow will be paused again when the downstream receives packets with the new `upstreamQ`. The old queue will likewise be unpaused when its last packet (that exceeded Th) departs the downstream switch.

To reduce the impact of such queue assignment changes, we add a timestamp to the flow table state, updated whenever a packet is enqueued or dequeued. A new queue assignment only happens if the `size` value in the flow table is 0, and the timestamp is older than a “sticky threshold” (i.e., the entry in the flow table has had no packets in the switch for at least this threshold). Since with BFC’s backpressure mechanism a flow can run out of packets for an $HRTT$, we set the sticky threshold to a small multiple of $HRTT$ ($2 HRTT$).

While sticky queue assignments reduce the chance that a backlogged flow will change queues, it doesn’t completely eliminate it (e.g., packets from the same flow may arrive slower than this interval due to an earlier bottleneck). Such situations are rare, and we found that BFC performs nearly identically to an ideal (but impractical) variant that pauses flows directly using the flow ID without sticky queue assignments.

4 SWITCHX IMPLEMENTATION

We implemented BFC in SwitchX, a to-be-released P4-based programmable switch ASIC with a Reconfigurable Match Table (RMT) architecture [14]. A packet in SwitchX first traverses

the ingress pipeline, followed by the traffic manager (TM) and finally the egress pipeline. SwitchX has four ingress and four egress RMT pipelines. Each pipeline has multiple stages, each capable of doing stateful packet operations. Ingress/egress ports are statically assigned to pipelines.

Bookkeeping: The flow table and pause counter are both maintained in the ingress pipeline. The flow table contains three values for each entry and is thus implemented as three separate register arrays (one for each value), updated one after the other.

Multiple pipelines: The flow table is *split* across the four ingress pipelines, and the size of the table in each ingress pipeline is $25 \times$ the number of queues. During normal operation, packets of an active flow arrive at a single ingress pipeline (same ingress port). Since the state for a flow only needs to be accessed in a single pipeline, we can split the flow table. However, splitting can marginally increase collisions if the incoming flows are distributed unevenly among the ingress pipelines. Similarly, the pause counter is split among the ingress pipelines. An ingress pipeline contains the pause counter entries corresponding to its own ingress ports.

Gathering queue depth information: We need queue depth information in the ingress pipeline for pausing and dynamic queue assignment. SwitchX has an inbuilt feature tailored for this task. The TM can communicate the queue depth information for all the queues in the switch to all the ingress pipelines without consuming any additional ingress cycles or bandwidth. The bitmap of empty queues is periodically updated with this data, with a different rotating starting point per pipeline to avoid new flows from being assigned to the same empty queue.

Communicating from egress to ingress pipeline: The enqueue operations described earlier are executed in the ingress pipeline when a packet arrives. Dequeue operations should happen at the egress but the bookkeeping data structures are at the ingress. To solve this, in the egress pipeline, we mirror packets as they exit and recirculate the header of the mirrored packet back to the ingress pipeline it came from. The dequeue operations are executed on the recirculated packet header.

Recirculating packets involves two constraints. First, the switch has dedicated internal links for recirculation, but the recirculation bandwidth is limited to 12% of the entire switch capacity. Second, the recirculated packet consumes an additional ingress cycle. The switch has a cap on the number of packets it can process every second (pps capacity).

Most workloads have an average packet size greater than 500 bytes [13], and SwitchX is designed with enough spare capacity in bandwidth and pps to handle header recirculation for every packet for those workloads (with room to spare). If the average packet size is much smaller, we can reduce recirculations by sampling packets for recirculation (described in App. E.1).

Recirculation is not fundamental to BFC. For example, SwitchX has native support for PFC bookkeeping in the TM. Likewise, if BFC bookkeeping was implemented in the TM, it would not need recirculation. Similarly, in switches with a disaggregated RMT architecture [20] where the same memory

can be accessed at both the ingress and egress, there is no need for recirculation.

5 DISCUSSION

Guaranteed losslessness. BFC does not guarantee losslessness. In particular, a switch in BFC pauses an `upstreamQ` only after receiving a packet from it. This implies an `upstreamQ` can send packets for up to an *HRTT* to the bottleneck switch before being paused, even if the switch is congested. In certain mass incast scenarios, this might be sufficient to trigger drops. Using credits [9, 36] could address this at the cost of added complexity. We leave an investigation of such prospective variants of BFC to future work. In our evaluation with realistic switch buffer sizes, BFC never incurred drops except under a 2000-to-1 incast (§6.2.3) and even then only 0.007% of the packets were dropped.

Deadlocks: Pushback mechanisms like PFC have been shown to be vulnerable to deadlocks in the presence of cyclic buffer dependencies (CBD) or misbehaving NICs [26, 28]. BFC NICs do not generate any backpressure and as a result cannot cause deadlocks. Since NICs always drain, in the absence of CBD, BFC cannot have deadlocks (see App. B for a formal proof). A downstream switch in BFC *will* resume an `upstreamQ` if it drains all the packets sent by the `upstreamQ`. If a downstream is not deadlocked, it will eventually drain packets from the upstream, and as a result, the corresponding upstream cannot be deadlocked.

To prevent CBD, we can reuse prior approaches for deadlock prevention. These approaches can be classified into two categories. The first is to redesign routing protocols to avoid installing routes that might cause CBD [52, 53]. The other is to identify a subset of possible ingress/egress pairs that are provably CBD free, and only send pause/resume along those pairs [29]. For a fat-tree topology, this would allow up-down paths but not temporary loops or detour routes [39]. In BFC, we use the latter approach. Given a topology, we pre-compute a match action table indexed by the ingress and egress port, and simply elide the backpressure pause/resume signal if it is disallowed. See App. B for details.

Incremental Deployment: In a full deployment, BFC would not require end-to-end congestion control. In a partial deployment, we advocate some form of end-to-end congestion control, such as capping the number of inflight packets of a flow. A common upgrade strategy is to upgrade switches more rapidly than server NICs. If only switches and not NICs are running BFC, capping inflight packets prevents a source NIC from overrunning the buffers of the first hop switch. The same strategy can be used for upgrading one cluster’s switches before the rest of the data center [58]. In our evaluation, we show incremental deployment would have some impact on buffer occupancy at the edge but minimal impact on performance (App. E.1).

6 EVALUATION

We present a proof-of-concept evaluation of our SwitchX implementation. To compare performance of BFC against existing schemes, we perform large scale ns-3 [3] simulations.

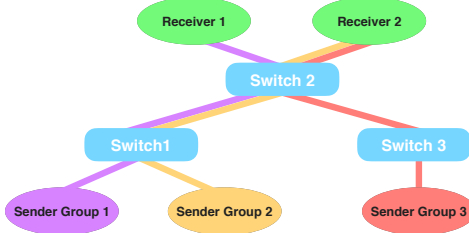


Figure 6: **Testbed topology.** The colored lines show the path for different flow groups.

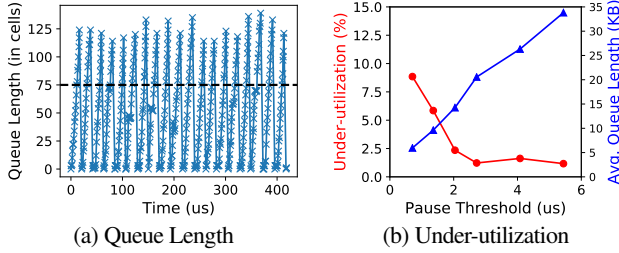


Figure 7: **Queue length and under-utilization.** 2 flows are competing at a 100 Gbps link. BFC achieves high utilization and low buffering.

6.1 SwitchX evaluation

Testbed: For evaluation, we were able to gain remote access to a SwitchX switch. Using a single switch, we created a simple multi-switch topology (Fig. 6) by looping back packets from the egress port back into the switch. All the ports are 100 Gbps, each port has 16 queues.⁴ The experiments include three groups of flows.

- Sender Group 1 \rightarrow Switch 1 \rightarrow Switch 2 \rightarrow Receiver 1.
- Sender Group 2 \rightarrow Switch 1 \rightarrow Switch 2 \rightarrow Receiver 2.
- Sender Group 3 \rightarrow Switch 3 \rightarrow Switch 2 \rightarrow Receiver 2.

To generate traffic we use the on-chip packet generator with no end-to-end congestion control.

Low buffering, high utilization: Fig. 7a shows the queue length for a flow when two flows are competing at a link (a group 2 flow is competing with a group 3 flow at the switch 2 \rightarrow receiver 2 link). The pause threshold is shown as a horizontal black line. BFC’s pausing mechanism is able to limit the queue length near the pause threshold (Th). The overshoot from Th is for two reasons. First, it takes an $HRTT$ for the pause to take effect. Second, SwitchX has small hardware queues after the egress pipeline, and a pause from the downstream cannot pause packets already in these hardware queues.

Notice that the queue length goes to 0 temporarily. Recall that a downstream switch only resumes the `upstreamQ` when it has drained all the packets from the `upstreamQ` that exceeded Th . As a result, a flow at the downstream can run out of packets for an $HRTT$. This can cause under-utilization when the queues for the two flows go empty simultaneously. We repeat the above experiment but vary the pause threshold. Fig. 7b shows the average queue length and the under-utilization of the congested link. With a pause threshold of 2 μs , BFC achieves close to 100% utilization with an average queue length of 15 KB.

⁴For 100 Gbps ports, SwitchX has 32 queues, but in loopback mode only 16 queues are available.

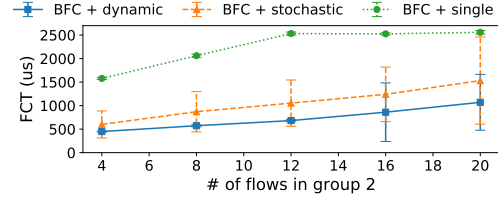


Figure 8: **Congestion spreading.** Dynamic queue assignment reduces HoL-blocking, improving FCTs on average and at the tail.

Queue assignment and congestion spreading: We next evaluate the impact of queue assignment on HoL-blocking and performance. We evaluate three different queue assignment strategies with BFC’s backpressure mechanism: (1) “BFC + single”: All flows are assigned to a single queue (similar to PFC); (2) “BFC + stochastic”: Flows are assigned to queues using stochastic hashing; (3) “BFC + dynamic”: Dynamic queue assignment as described in §3.3.1.

The setup consists of two group 1 flows, eight group 3 flows, and a number of group 2 flows varied between four to twenty. All flows are 1.5 MB in size. The experiment is designed such that for group 2 and 3 flows, the bottleneck is the switch 2 \rightarrow receiver 2 link. The bottleneck for group 1 flows is the switch 1 \rightarrow switch 2 link. Switch 2 will pause queues at switch 1 in response to congestion from group 2 flows. Notice that group 1 and group 2 flows are sharing the switch 1 \rightarrow switch 2 link. If a group 1 flow shares a queue with a group 2 flow (a collision), the backpressure due to the group 2 flow can slow down the group 1 flow, causing HoL-blocking and increasing its flow completion time (FCT) unnecessarily.

Fig. 8 shows the average FCT for group 1 flows across four runs. The whiskers correspond to one standard deviation in the FCT. BFC + single achieves the worst FCT as group 1 and 2 flows always share a queue. With stochastic assignment, the FCT is substantially lower, but the standard deviation in FCT is high. In some runs, group 1 and 2 flows don’t share a queue and there is no HoL-blocking. In other runs, due to the stochastic nature of assignment, they do share a queue (even when there are other empty queues), resulting in worse performance. With dynamic assignment, BFC achieves the lowest average FCT and the best tail performance. In particular, the standard deviation is close to 0 when the number of flows at the switch 1 \rightarrow switch 2 link (group 1 + group 2 flows) is lower than the number of queues. In such scenarios, group 1 flows consistently incur no collisions. When the number of flows exceed the queues, collisions are inevitable, and the standard deviation in FCT increases.

6.2 Simulation-based evaluation

We also implemented BFC in ns-3 [3]. For DCQCN we use [4], and for all other schemes we use [2].

6.2.1 Setup

Network Topology: We use a Clos topology with 128 leaf servers, 8 top of the rack (ToR) switches and 8 Spine switches (2:1 over subscription). Each Spine switch is connected to all the ToR switches, each ToR has 16 servers, and each server

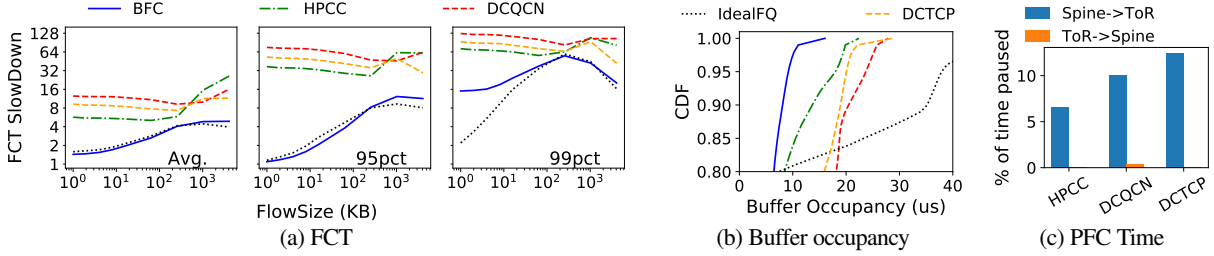


Figure 9: Google distribution with 55% load + 5% 100-1 incast. BFC tracks the ideal behavior, improves FCTs, and reduces buffer occupancy. For FCT slowdown, both the x and y axis are log scaled.

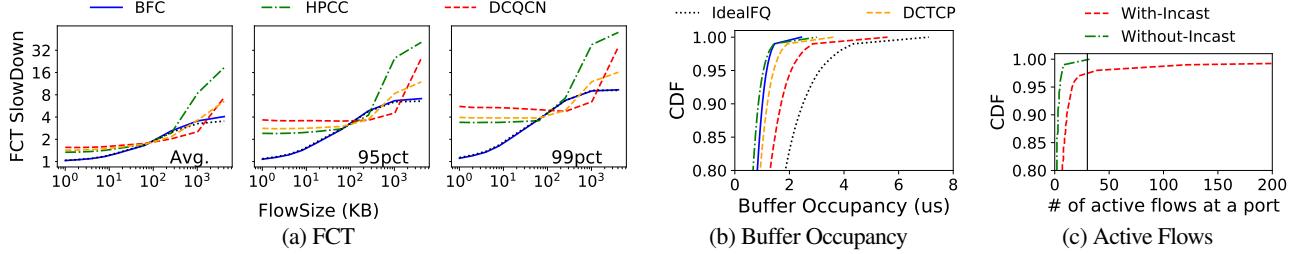


Figure 10: FCT slowdown and buffer occupancy for Google distribution with 60% load. For all the schemes, PFC was never triggered. Fig. 10c shows the CDF of active flows at a port with and without incast. The vertical line shows the total number of queues per port.

is connected to a single ToR. All links are 100Gbps with a propagation delay of 1 μ s. The maximum end-to-end base round trip time (RTT) is 8 μ s and the 1-Hop RTT is 2 μ s. The switch buffer size is set to 12 MB. Relative to the ToR switch capacity of 2.4 Tbps, the ratio of buffer size to switch capacity is 40 μ s, the same as Broadcom’s Tomahawk3 from Fig. 1. We use an MTU of 1KB and unless specified otherwise we use Go-Back-N for retransmission. Our experiments use the shared buffer memory model, common in existing switches [17]. We use flow-level ECMP for all the schemes.

Comparison: *HPCC*: HPCC is an end-to-end control algorithm that uses explicit link utilization information from the switches to reduce buffer occupancy and drops/PFCs at the congested switch. We use the parameters from the paper, $\eta = 0.95$ and $maxStage = 5$. The dynamic PFC threshold is set to trigger when traffic from an input port occupies more than 11% of the free buffer (as in the HPCC paper). We use the same PFC thresholds for DCQCN and DCTCP.

DCQCN: DCQCN uses ECN bits and end-to-end control to manage buffer use at the congested switch. The ECN threshold triggers before PFC ($K_{min} = 100KB$ and $K_{max} = 400KB$).

DCTCP: The ECN threshold is same as DCQCN. Flows start at line rate to avoid degradation in FCTs from slow-start.

BFC: We use 32 physical queues per port (consistent with SwitchX) and our flow table has 76K entries. The flow table takes 400 KB of memory. We chose per-flow fair queuing as our scheduling mechanism; all the comparison schemes strive for per-flow fairness, thus, fair queuing provides for a just comparison.

Ideal-FQ: To understand how close BFC comes to optimal performance, we simulate ideal fair queuing with infinite buffering at each switch. The NICs cap the in-flight packets of a flow to 1 BDP. Note that infinite buffering is not realizable in practice; its role is to bound how well we might possibly do on FCTs.

Performance metrics: We consider three performance metrics: (1) FCT normalized to the best possible FCT for the same size flow, running at link rate (referred as the FCT slowdown); (2) Overall buffer occupancy at the switch; (3) Throughput of individual flows.

Workloads: We synthesized a trace to match the flow size distributions from the industry workloads discussed in Fig. 2: (1) Aggregated workload from all applications in a Google data center; (2) a Hadoop cluster at Facebook (FB_Hadoop). The flow arrival pattern is open-loop and follows a *bursty* lognormal inter-arrival-time distribution with $\sigma = 2$. For each flow arrival, the source-destination pair is derived from a uniform distribution. We consider scenarios with and without incast, different traffic load settings, and incast ratios. Since our topology is oversubscribed, on average links in the core (Spine-ToR) will be more congested than the ToR-leaf server links. In our experiments, by X% load we mean X% load on the links in the core.

6.2.2 Performance

Fig. 9 and 10 show our principal results. The flow sizes are drawn from the Google distribution and the average load is set to 60% of the network capacity. For Fig. 9 (but not Fig. 10), 5% of the traffic (on average) is from incast flows. The incast degree is 100-to-1 and the size is 20MB in aggregate. A new incast event starts every 500 μ s. Since the best-case completion time for an incast is 1.6 ms (20 MB/100 Gbps), multiple incasts coexist simultaneously in the network. We report the tail buffer occupancy, the FCT slowdowns at the average, 95th and 99th percentile, and the fraction of time links were paused due to PFC. We report the FCT slowdowns for the incast traffic separately in App. C.

Out of all the schemes, DCQCN is worst on latency for small flow sizes, both at the average and the tail. Compared to DCQCN, DCTCP improves latency as it uses per-ACK feedback instead of periodic feedback via QCN. However, the frequent

feedback is not enough, and the performance is far from optimal (Ideal-FQ). The problem is that both DCQCN and DCTCP are slow in responding to congestion. Since flows start at line rate, a flow can build up an entire end-to-end bandwidth-delay product (BDP) of buffering (100 KB) at the bottleneck before there is any possibility of reducing its rate. The problem is aggravated during incast events. The bottleneck switch can potentially accumulate one BDP of packets per incast flow (10MB in aggregate for 100-to-1 incast).

Both protocols have low throughput for long flows. When capacity becomes available, a long flow may fail to ramp up quickly enough, reducing throughput and shifting its work to busier periods where it can impact other flows. Moreover, on sudden onset of congestion, a flow may not reduce its rate fast enough, slowing short flows.

HPCC improves on DCQCN and DCTCP by using link utilization instead of ECN and a better control algorithm. Compared to DCQCN and DCTCP, HPCC reduces tail latency, tail buffer occupancy, and PFC pauses (in case of incast). Compared to BFC, however, HPCC has $5\text{-}30\times$ worse tail latency for short flows with incast, and $2.3\text{-}3\times$ worse without. Long flows do worse with HPCC than DCQCN and DCTCP. HPCC aims to maintain small buffers to improve tail latency for short flows, and this means the switch can run out of packets before the flows ramp up when bandwidth becomes available.

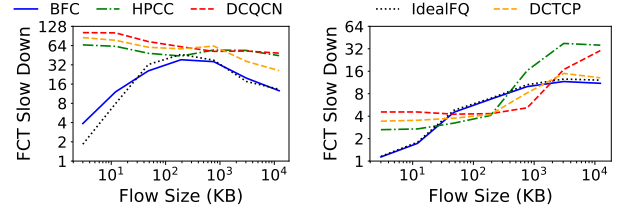
Ideal-FQ achieves lower latency than all the schemes. However, buffer occupancy can grow to an unfeasible level.

BFC achieves the best latency (both average and tail) among all the schemes. Without incast, BFC performance closely tracks optimal. With incast, incoming flows exhaust the number of physical queues, triggering HoL-blocking and hurting tail latency. This effect is largest for the smallest flows at the tail. Fig. 10c shows the average number of active flows at a port. In the absence of incast, the number of active flows is smaller than the total queues 99% of the time, and collisions are rare. With incast, the number of active flows increase, causing collisions. However, the tail latency for short flows with BFC is still $5\text{-}30\times$ better than existing schemes. BFC also improves the performance of incast flows, achieving $2\times$ better FCTs at the tail compared to HPCC (see App. C).

In the absence of incast, the buffer occupancy for HPCC is similar to that of BFC, but this low buffering comes at the cost of link under-utilization and high FCT for long flows.

Note that, compared to BFC and Ideal-FQ, latency for medium flows (200-1000KB) is slightly better with existing schemes. Because they slow down long flows relative to perfect fairness, medium flows have room to get through more quickly. Conversely, tail slowdown is better for long flows than medium flows with BFC and Ideal-FQ. Long flows achieve close to the long term average available bandwidth, while medium flows are more affected by transient congestion.

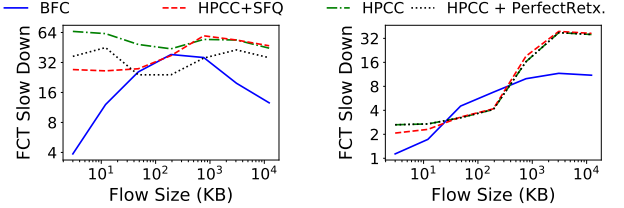
We repeated the experiment in Fig. 9 and 10 with the Facebook distribution. Fig. 11 shows the 99th percentile FCT slowdown. The trends in the FCT slowdowns are similar to that



(a) 55% + 5% 100-1 incast

(b) 60%

Figure 11: FCT slowdown (99th percentile) for Facebook distribution with and without incast.



(a) 55% + 5% incast

(b) 60%

Figure 12: FCT slowdown (99th percentile) of HPCC variants, using the setup in Fig. 11.

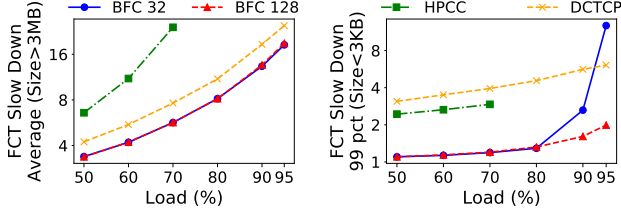
of the Google distribution. We omit other statistics presented earlier in the interest of space, but the trends are similar to Fig. 9 and 10. Note that the x-axis in Fig. 11 from Fig. 9 and 10 because the flow size distribution is different. Henceforth, all the experiments use the Facebook workload.

Comparison with HPCC and DCTCP variants: To better understand the benefits of BFC, we added advanced features to HPCC and repeated the experiment in Fig. 11. Fig. 12 reports the FCTs with these variants. We also show BFC and the original HPCC (with PFC) in the results.

Scheduling: First, we evaluate HPCC+SFQ, a scheme that combines HPCC with better scheduling at the switch. Each egress port does stochastic fair queuing on incoming flows. To match BFC we use 32 physical queues. Adding scheduling improves tail latency by allowing different flows to be scheduled from different physical queues. However, the FCT slowdowns are still worse than BFC, because: (i) There are collisions in assigning flows to physical queues. A small flow sharing the queue with other flows will see its packets delayed. (ii) Regardless of scheduling, HPCC adjusts rates in an end-to-end manner, leading to poor control of buffer occupancy and low throughput for long flows. In particular, with incast, HPCC+SFQ builds deep buffers and experiences PFC pauses at the same rate as HPCC, both of which hurt latency.

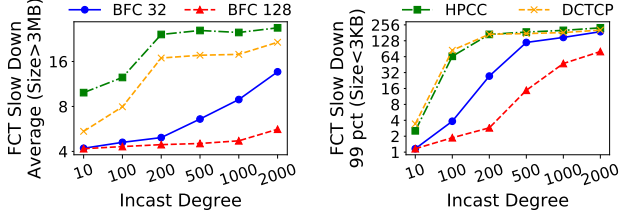
Retransmission: Next, we replace PFC in HPCC with perfect retransmission. Without incast, the performance is identical to HPCC as PFC is never triggered in this scenario. With incast, HPCC + Perfect Retransmission improves performance compared to HPCC but is still far from BFC. Retransmission on its own doesn't reduce buffer occupancy, but it does help tail latency of medium flows with incast.

Slow-start: We also evaluate the impact of using TCP slow-start instead of starting flows at line rate. We compare the original DCTCP with slow start (DCTCP + SS) and our modified DCTCP where flows start at the line rate. With incast, DCTCP + SS re-



(a) Average FCT for long flows (b) Tail FCT for short flows

Figure 13: Average FCT slowdown for long flows, and 99th percentile tail FCT slowdown for small flows, as a function of load.



(a) Average FCT for long flows (b) Tail FCT for short flows

Figure 14: Average FCT slowdown for long flows, and 99th percentile tail FCT slowdown for small flows, as a function of incast degree.

duces buffer occupancy by reducing the intensity of incast flows, improving tail latency. However, it also increases median FCTs by up to $2\times$. Flows start at a lower rate, taking longer to ramp up to the desired rate. In the absence of incast, it increases both the tail and median FCT for short flows. See App. D for details.

6.2.3 Stress-testing BFC

In this section we stress-test BFC under high load and large incast degree. Flow arrivals follow a bursty lognormal distribution ($\sigma = 2$). We evaluate BFC under two different queue configurations: (1) 32 queues per port (BFC 32); (2) 128 queues per port (BFC 128). We show the average slowdown for long flows ($> 3\text{MB}$) and 99th percentile slowdown for short flows ($< 3\text{KB}$).

Load: Fig. 13 shows the performance as we vary the average load from 50 to 95% (without incast). HPCC only supports loads up to 70%. At higher loads, it becomes unstable (the number of outstanding flows grows without bound), in part due to the overhead of the INT header (80 B per-packet). All other schemes were stable across all load values.

At loads $\leq 80\%$, BFC 32 achieves both lower tail latency (Fig. 13b) for short flows and higher throughput for long flows (Fig. 13a). The tail latency for short flows is close to the perfect value of 1. At higher loads, flows remain queued at the bottleneck switch for longer periods of time, raising the likelihood that we run out of physical queues, leading to head of line blocking. This particularly hurts tail performance for short flows as they might be delayed for an extended period if they are assigned to the same queue as a long flow. At the very high load of 95%, the HoL-blocking degrades tail latency substantially for BFC 32. However, it still achieves good link utilization, and the impact of collisions is limited for long flows.

Increasing queues, reduces collisions and the associated HoL-blocking. BFC 128 achieves better tail latency for short flows at load $\geq 90\%$.

Incast degree: If the size of an incast is large enough, it can exhaust physical queues and hurt performance. Fig. 14 shows the effect of varying the degree of incast on performance. The average load is 60% and includes a 5% incast. The incast size is 20MB in aggregate, but we vary the degree of incast from 10 to 2000.

For throughput, both BFC 32 and BFC 128 perform well as long as the incast degree is moderate compared to the number of queues. Both start to degrade around $15\times$ the number of queues per port. Below this, BFC can leverage the fanin from the larger number of upstream queues (and greater aggregate upstream buffer space) to keep the incast from impeding unrelated traffic (§3.3.1). As the incast degree scales up farther, BFC 32 is able to retain some of its advantage relative to HPCC and DCTCP.

For high incast degree, the tail latency for short flows converges to that of HPCC and DCTCP (Fig. 14b). The tail is skewed by the few percent of small requests that happen to go to the same destination as the incast. (Across the 128 leaf servers in our setup, several servers are the target of an incast at any one time, and these also receive their share of normal traffic.) As the incast degree increases, more small flows share physical queues with incast flows, leading to more HoL-blocking.

6.2.4 Additional experiments

Incremental Deployment: We repeated the experiment in Fig. 11a in the scenario where (i) BFC is deployed in part of the network; (ii) The switch doesn't have enough capacity to handle all the recirculations. The impact on FCTs is minimal under these scenarios (see App. E.1).

Impact of scheduling policy: The design of BFC is orthogonal to the scheduling policy. We repeat the experiment in Fig. 11, but change the scheduling policy from fair queuing (FQ) to shortest remaining flow first (SRF). With SRF, BFC reduces FCTs by prioritizing short flows (see App. E.2).

Performance in asymmetric topologies: BFC makes no assumption about the topology, link speeds and link delays. We evaluate the performance of BFC in a multi-datacenter topology. BFC achieves low FCT for flows within the datacenter, and high link utilization for the inter-datacenter links (see App. E.3).

Importance of dynamic queue assignment: We repeat the experiment in Fig. 11a but use stochastic hashing to statically assign flows to physical queue instead. With stochastic assignment, collisions in physical queue increase, hurting FCTs (see App. E.4).

Size of flow table: Reducing the size of the flow table can increase index collisions in the flow table, potentially hurting FCTs. We repeat the experiment in Fig. 11a and evaluate the impact of size of flow table. Reducing the size impacts the short flow FCTs partly (see App. E.5).

Reducing contention for queues: We tried a variant of BFC where the sender labels incast flows explicitly (similar to [44]). All the incast flows at an egress port are assigned to the same queue. This frees up queues for non-incast traffic and reduces collisions substantially under large incasts. (see App. E.6).

7 CONCLUSION

In this paper, we present Backpressure Flow Control (BFC), a practical congestion control architecture for datacenter networks. BFC provides per-hop per-flow flow control, but with bounded state, constant-time switch operations, and careful use of buffers. Switches dynamically assign flows to physical queues, allowing fair scheduling among competing flows and use selective backpressure to reduce buffering with minimal head of line blocking. Relative to existing end-to-end congestion control schemes, BFC improves short flow tail latency and long flow utilization for networks with high bandwidth links and bursty traffic. We demonstrate BFC's feasibility by implementing it on a state-of-art P4-based programmable hardware switch. In simulation, compared to existing end-to-end schemes, BFC achieves $2.3\text{--}60\times$ lower tail latency for short flows and $1.6\text{--}5\times$ better average completion time for long flows.

REFERENCES

- [1] Birthday problem. https://en.wikipedia.org/wiki/Birthday_problem.
- [2] Hpcc simulation. <https://github.com/alibaba-edu/High-Precision-Congestion-Control>.
- [3] Network simulator 3. <https://www.nsnam.org>.
- [4] Ns-3 simulator for rdma. <https://github.com/bobzhuyb/ns3-rdma>.
- [5] Atul Adya, Robert Grandl, Daniel Myers, and Henry Qin. Fast key-value stores: An idea whose time has come and gone. In *Proceedings of the Workshop on Hot Topics in Operating Systems, HotOS 2019, Bertinoro, Italy, May 13-15, 2019*, pages 113–119. ACM, 2019.
- [6] Mohammad Alizadeh, Albert G. Greenberg, David A. Maltz, Jitendra Padhye, Parveen Patel, Balaji Prabhakar, Sudipta Sengupta, and Murari Sridharan. Data center TCP (DCTCP). In Shivkumar Kalyanaraman, Venkata N. Padmanabhan, K. K. Ramakrishnan, Rajeev Shorey, and Geoffrey M. Voelker, editors, *Proceedings of the ACM SIGCOMM 2010 Conference on Applications, Technologies, Architectures, and Protocols for Computer Communications, New Delhi, India, August 30 -September 3, 2010*, pages 63–74. ACM, 2010.
- [7] Mohammad Alizadeh, Shuang Yang, Milad Sharif, Sachin Katti, Nick McKeown, Balaji Prabhakar, and Scott Shenker. pfabric: minimal near-optimal datacenter transport. In Dah Ming Chiu, Jia Wang, Paul Barford, and Srinivasan Seshan, editors, *ACM SIGCOMM 2013 Conference, SIGCOMM'13, Hong Kong, China, August 12-16, 2013*, pages 435–446. ACM, 2013.
- [8] Amazon. Amazon Web Services. <https://aws.amazon.com/s3/>.
- [9] Thomas E. Anderson, Susan S. Owicki, James B. Saxe, and Charles P. Thacker. High speed switch scheduling for local area networks. *ACM Trans. Comput. Syst.*, 11(4):319–352, 1993.
- [10] Arista. Arista 7170 Multi-function Programmable Networking. https://www.arista.com/assets/data/pdf/Whitepapers/7170_White_Paper.pdf.
- [11] Tom Barbette, Chen Tang, Haoran Yao, Dejan Kostic, Gerald Q. Maguire Jr., Panagiotis Papadimitratos, and Marco Chiesa. A high-speed load-balancer design with guaranteed per-connection-consistency. In Ranjita Bhagwan and George Porter, editors, *17th USENIX Symposium on Networked Systems Design and Implementation, NSDI 2020, Santa Clara, CA, USA, February 25-27, 2020*, pages 667–683. USENIX Association, 2020.
- [12] Barefoot. Tofino: World's Fastest P4-Compatible Ethernet Switch ASICs. <https://www.barefootnetworks.com/products/brief-tofino/>.
- [13] Theophilus Benson, Ashok Anand, Aditya Akella, and Ming Zhang. Understanding data center traffic characteristics. *Comput. Commun. Rev.*, 40(1):92–99, 2010.
- [14] Pat Bosshart, Dan Daly, Glen Gibb, Martin Izzard, Nick McKeown, Jennifer Rexford, Cole Schlesinger, Dan Talayco, Amin Vahdat, George Varghese, and David Walker. P4: programming protocol-independent packet processors. *Comput. Commun. Rev.*, 44(3):87–95, 2014.
- [15] Pat Bosshart, Glen Gibb, Hun-Seok Kim, George Varghese, Nick McKeown, Martin Izzard, Fernando Mujica, and Mark Horowitz. Forwarding metamorphosis: Fast programmable match-action processing in hardware for sdn. In *Proceedings of the ACM SIGCOMM 2013 Conference, SIGCOMM'13*, page 99–110, New York, NY, USA, 2013. Association for Computing Machinery.
- [16] Eric A. Brewer and Bradley C. Kuszmaul. How to get good performance from the CM-5 data network. In Howard Jay Siegel, editor, *Proceedings of the 8th International Symposium on Parallel Processing, Cancún, Mexico, April 1994*, pages 858–867. IEEE Computer Society, 1994.
- [17] Broadcom. StrataXGS. <https://www.broadcom.com/products/ethernet-connectivity/switching/strataxgs>.
- [18] Neal Cardwell, Yuchung Cheng, C. Stephen Gunn, Soheil Hassas Yeganeh, and Van Jacobson. BBR: Congestion-Based Congestion Control. *ACM Queue*, 14(5):50:20–50:53, October 2016.
- [19] Inho Cho, Keon Jang, and Dongsu Han. Credit-scheduled delay-bounded congestion control for datacenters. In *Proceedings of the Conference of the ACM Special Interest*

Group on Data Communication, SIGCOMM 2017, Los Angeles, CA, USA, August 21-25, 2017, pages 239–252. ACM, 2017.

- [20] Sharad Chole, Andy Fingerhut, Sha Ma, Anirudh Sivaraman, Shay Vargaftik, Alon Berger, Gal Mendelson, Mohammad Alizadeh, Shang-Tse Chuang, Isaac Keslassy, Ariel Orda, and Tom Edsall. drmt: Disaggregated programmable switching. In *Proceedings of the Conference of the ACM Special Interest Group on Data Communication, SIGCOMM 2017, Los Angeles, CA, USA, August 21-25, 2017*, pages 1–14. ACM, 2017.
- [21] Jeffrey Dean and Luiz André Barroso. The tail at scale. *Commun. ACM*, 56(2):74–80, 2013.
- [22] Sally Floyd, Jamshid Mahdavi, Matt Mathis, and Matthew Podolsky. An extension to the selective acknowledgement (SACK) option for TCP. *RFC*, 2883:1–17, 2000.
- [23] Peter Xiang Gao, Akshay Narayan, Gautam Kumar, Rachit Agarwal, Sylvia Ratnasamy, and Scott Shenker. phost: distributed near-optimal datacenter transport over commodity network fabric. In Felipe Huici and Giuseppe Bianchi, editors, *Proceedings of the 11th ACM Conference on Emerging Networking Experiments and Technologies, CoNEXT 2015, Heidelberg, Germany, December 1-4, 2015*, pages 1:1–1:12. ACM, 2015.
- [24] Google. Google Cloud Platform. <https://cloud.google.com>.
- [25] Matthew P. Grosvenor, Malte Schwarzkopf, Ionel Gog, Robert N. M. Watson, Andrew W. Moore, Steven Hand, and Jon Crowcroft. Queues don’t matter when you can JUMP them! In *12th USENIX Symposium on Networked Systems Design and Implementation, NSDI 15, Oakland, CA, USA, May 4-6, 2015*, pages 1–14. USENIX Association, 2015.
- [26] Chuanxiong Guo, Haitao Wu, Zhong Deng, Gaurav Soni, Jianxi Ye, Jitu Padhye, and Marina Lipshteyn. RDMA over commodity ethernet at scale. In Marinho P. Barcellos, Jon Crowcroft, Amin Vahdat, and Sachin Katti, editors, *Proceedings of the ACM SIGCOMM 2016 Conference, Florianopolis, Brazil, August 22-26, 2016*, pages 202–215. ACM, 2016.
- [27] Mark Handley, Costin Raiciu, Alexandru Agache, Andrei Voinescu, Andrew W. Moore, Gianni Antichi, and Marcin Wójcik. Re-architecting datacenter networks and stacks for low latency and high performance. In *Proceedings of the Conference of the ACM Special Interest Group on Data Communication, SIGCOMM 2017, Los Angeles, CA, USA, August 21-25, 2017*, pages 29–42. ACM, 2017.
- [28] Shuihai Hu, Yibo Zhu, Peng Cheng, Chuanxiong Guo, Kun Tan, Jitendra Padhye, and Kai Chen. Deadlocks in datacenter networks: Why do they form, and how to avoid them. In Bryan Ford, Alex C. Snoeren, and Ellen W. Zegura, editors, *Proceedings of the 15th ACM Workshop on Hot Topics in Networks, HotNets 2016, Atlanta, GA, USA, November 9-10, 2016*, pages 92–98. ACM, 2016.
- [29] Shuihai Hu, Yibo Zhu, Peng Cheng, Chuanxiong Guo, Kun Tan, Jitendra Padhye, and Kai Chen. Tagger: Practical PFC deadlock prevention in data center networks. In *Proceedings of the 13th International Conference on emerging Networking EXperiments and Technologies, CoNEXT 2017, Incheon, Republic of Korea, December 12 - 15, 2017*, pages 451–463. ACM, 2017.
- [30] Lavanya Jose, Stephen Ibanez, Mohammad Alizadeh, and Nick McKeown. A distributed algorithm to calculate max-min fair rates without per-flow state. *Proc. ACM Meas. Anal. Comput. Syst.*, 3(2):21:1–21:42, 2019.
- [31] Changhoon Kim, Anirudh Sivaraman, Naga Katta, Antonin Bas, Advait Dixit, and Lawrence J Wobker. In-band network telemetry via programmable dataplanes. 2015.
- [32] Leonard Kleinrock. *Queueing systems, volume 2: Computer applications*, volume 66. wiley New York, 1976.
- [33] Smaragda Konstantinidou and Lawrence Snyder. Chaos router: Architecture and performance. In Zvonko G. Vranesic, editor, *Proceedings of the 18th Annual International Symposium on Computer Architecture. Toronto, Canada, May, 27-30 1991*, pages 212–221. ACM, 1991.
- [34] Abdesslem Kortebi, Luca Muscariello, Sara Oueslati, and James W. Roberts. Evaluating the number of active flows in a scheduler realizing fair statistical bandwidth sharing. In Derek L. Eager, Carey L. Williamson, Sem C. Borst, and John C. S. Lui, editors, *Proceedings of the International Conference on Measurements and Modeling of Computer Systems, SIGMETRICS 2005, June 6-10, 2005, Banff, Alberta, Canada*, pages 217–228. ACM, 2005.
- [35] Gautam Kumar, Nandita Dukkupati, Keon Jang, Hassan M. G. Wassel, Xian Wu, Behnam Montazeri, Yaogong Wang, Kevin Springborn, Christopher Alfeld, Michael Ryan, David Wetherall, and Amin Vahdat. Swift: Delay is simple and effective for congestion control in the datacenter. In Henning Schulzrinne and Vishal Misra, editors, *SIGCOMM ’20: Proceedings of the 2020 Annual conference of the ACM Special Interest Group on Data Communication on the applications, technologies, architectures, and protocols for computer communication, Virtual Event, USA, August 10-14, 2020*, pages 514–528. ACM, 2020.
- [36] NT Kung and Robert Morris. Credit-based flow control for ATM networks. *IEEE network*, 9(2):40–48, 1995.

- [37] Daniel Lenoski, James Laudon, Kourosh Gharachorloo, Wolf-Dietrich Weber, Anoop Gupta, John L. Hennessy, Mark Horowitz, and Monica S. Lam. The stanford dash multiprocessor. *Computer*, 25(3):63–79, 1992.
- [38] Yuliang Li, Rui Miao, Hongqiang Harry Liu, Yan Zhuang, Fei Feng, Lingbo Tang, Zheng Cao, Ming Zhang, Frank Kelly, Mohammad Alizadeh, and Minlan Yu. HPCC: high precision congestion control. In Jianping Wu and Wendy Hall, editors, *Proceedings of the ACM Special Interest Group on Data Communication, SIGCOMM 2019, Beijing, China, August 19-23, 2019*, pages 44–58. ACM, 2019.
- [39] Vincent Liu, Daniel Halperin, Arvind Krishnamurthy, and Thomas E. Anderson. F10: A fault-tolerant engineered network. In Nick Feamster and Jeffrey C. Mogul, editors, *Proceedings of the 10th USENIX Symposium on Networked Systems Design and Implementation, NSDI 2013*, pages 399–412. USENIX Association, 2013.
- [40] Paul E. McKenney. Stochastic fairness queueing. In *Proceedings IEEE INFOCOM '90, The Conference on Computer Communications, Ninth Annual Joint Conference of the IEEE Computer and Communications Societies, The Multiple Facets of Integration, San Francisco, CA, USA, June 3-7, 1990*, pages 733–740. IEEE Computer Society, 1990.
- [41] Microsoft. Microsoft Azure. <https://azure.microsoft.com/>.
- [42] Radhika Mittal, Vinh The Lam, Nandita Dukkkipati, Emily R. Blem, Hassan M. G. Wassef, Monia Ghobadi, Amin Vahdat, Yaogong Wang, David Wetherall, and David Zats. TIMELY: rtt-based congestion control for the datacenter. In Steve Uhlig, Olaf Maennel, Brad Karp, and Jitendra Padhye, editors, *Proceedings of the 2015 ACM Conference on Special Interest Group on Data Communication, SIGCOMM 2015, London, United Kingdom, August 17-21, 2015*, pages 537–550. ACM, 2015.
- [43] Radhika Mittal, Alexander Shpiner, Aurojit Panda, Eitan Zahavi, Arvind Krishnamurthy, Sylvia Ratnasamy, and Scott Shenker. Revisiting network support for RDMA. In Sergey Gorinsky and János Tapolcai, editors, *Proceedings of the 2018 Conference of the ACM Special Interest Group on Data Communication, SIGCOMM 2018, Budapest, Hungary, August 20-25, 2018*, pages 313–326. ACM, 2018.
- [44] Behnam Montazeri, Yilong Li, Mohammad Alizadeh, and John K. Ousterhout. Homa: a receiver-driven low-latency transport protocol using network priorities. In Sergey Gorinsky and János Tapolcai, editors, *Proceedings of the 2018 Conference of the ACM Special Interest Group on Data Communication, SIGCOMM 2018, Budapest, Hungary, August 20-25, 2018*, pages 221–235. ACM, 2018.
- [45] The Next Platform. Flattening networks - and budgets - with 400G ethernet. <https://www.nextplatform.com/2018/01/20/flattening-networks-budgets-400g-ethernet/>. January 20, 2018.
- [46] Salvatore Pontarelli, Roberto Bifulco, Marco Bonola, Carmelo Cascone, Marco Spaziani, Valerio Bruschi, Davide Sanvito, Giuseppe Siracusano, Antonio Capone, Michio Honda, and Felipe Huici. Flowblaze: Stateful packet processing in hardware. In Jay R. Lorch and Minlan Yu, editors, *16th USENIX Symposium on Networked Systems Design and Implementation, NSDI 2019, Boston, MA, February 26-28, 2019*, pages 531–548. USENIX Association, 2019.
- [47] Ahmed Saeed, Varun Gupta, Prateesh Goyal, Milad Sharif, Rong Pan, Mostafa H. Ammar, Ellen W. Zegura, Keon Jang, Mohammad Alizadeh, Abdul Kabbani, and Amin Vahdat. Annulus: A dual congestion control loop for datacenter and WAN traffic aggregates. In Henning Schulzrinne and Vishal Misra, editors, *SIGCOMM '20: Proceedings of the 2020 Annual conference of the ACM Special Interest Group on Data Communication on the applications, technologies, architectures, and protocols for computer communication, Virtual Event, USA, August 10-14, 2020*, pages 735–749. ACM, 2020.
- [48] Naveen Kr. Sharma, Ming Liu, Kishore Atreya, and Arvind Krishnamurthy. Approximating fair queueing on reconfigurable switches. In Sujata Banerjee and Srinivasan Seshan, editors, *15th USENIX Symposium on Networked Systems Design and Implementation, NSDI 2018, Renton, WA, USA, April 9-11, 2018*, pages 1–16. USENIX Association, 2018.
- [49] Arjun Singh, Joon Ong, Amit Agarwal, Glen Anderson, Ashby Armistead, Roy Bannon, Seb Boving, Gaurav Desai, Bob Felderman, Paulie Germano, Anand Kanagala, Jeff Provost, Jason Simmons, Eiichi Tanda, Jim Wanderer, Urs Hölzle, Stephen Stuart, and Amin Vahdat. Jupiter rising: A decade of clos topologies and centralized control in google’s datacenter network. In Steve Uhlig, Olaf Maennel, Brad Karp, and Jitendra Padhye, editors, *Proceedings of the 2015 ACM Conference on Special Interest Group on Data Communication, SIGCOMM 2015, London, United Kingdom, August 17-21, 2015*, pages 183–197. ACM, 2015.
- [50] Anirudh Sivaraman, Alvin Cheung, Mihai Budiu, Changhoon Kim, Mohammad Alizadeh, Hari Balakrishnan, George Varghese, Nick McKeown, and Steve Licking. Packet transactions: High-level programming for line-rate switches. In Marinho P. Barcellos, Jon Crowcroft, Amin Vahdat, and Sachin Katti, editors, *Proceedings of the ACM SIGCOMM 2016 Conference, Florianopolis, Brazil, August 22-26, 2016*, pages 15–28. ACM, 2016.
- [51] Anirudh Sivaraman, Suvinay Subramanian, Mohammad Alizadeh, Sharad Chole, Shang-Tse Chuang, Anurag

- Agrawal, Hari Balakrishnan, Tom Edsall, Sachin Katti, and Nick McKeown. Programmable packet scheduling at line rate. In Marinho P. Barcellos, Jon Crowcroft, Amin Vahdat, and Sachin Katti, editors, *Proceedings of the ACM SIGCOMM 2016 Conference, Florianopolis, Brazil, August 22-26, 2016*, pages 44–57. ACM, 2016.
- [52] Brent Stephens and Alan L. Cox. Deadlock-free local fast failover for arbitrary data center networks. In *35th Annual IEEE International Conference on Computer Communications, INFOCOM 2016, San Francisco, CA, USA, April 10-14, 2016*, pages 1–9. IEEE, 2016.
- [53] Brent Stephens, Alan L. Cox, Ankit Singla, John B. Carter, Colin Dixon, and Wes Felter. Practical DCB for improved data center networks. In *2014 IEEE Conference on Computer Communications, INFOCOM 2014, Toronto, Canada, April 27 - May 2, 2014*, pages 1824–1832. IEEE, 2014.
- [54] Robert Williams and Bahadir Erimli. Method and apparatus for performing priority-based flow control, October 18 2005. US Patent 6,957,269.
- [55] Xiaowei Yang, David Wetherall, and Thomas E. Anderson. TVA: a dos-limiting network architecture. *IEEE/ACM Trans. Netw.*, 16(6):1267–1280, 2008.
- [56] David Zats, Tathagata Das, Prashanth Mohan, Dhruba Borthakur, and Randy H. Katz. Detail: reducing the flow completion time tail in datacenter networks. In Lars Eggert, Jörg Ott, Venkata N. Padmanabhan, and George Varghese, editors, *ACM SIGCOMM 2012 Conference, SIGCOMM '12, Helsinki, Finland - August 13 - 17, 2012*, pages 139–150. ACM, 2012.
- [57] Xin Zhang, Hsu-Chun Hsiao, Geoffrey Hasker, Haowen Chan, Adrian Perrig, and David G. Andersen. SCION: scalability, control, and isolation on next-generation networks. In *32nd IEEE Symposium on Security and Privacy, S&P 2011, 22-25 May 2011, Berkeley, California, USA*, pages 212–227. IEEE Computer Society, 2011.
- [58] Shizhen Zhao, Rui Wang, Junlan Zhou, Joon Ong, Jeffrey C. Mogul, and Amin Vahdat. Minimal rewiring: Efficient live expansion for clos data center networks. In Jay R. Lorch and Minlan Yu, editors, *16th USENIX Symposium on Networked Systems Design and Implementation, NSDI 2019, Boston, MA, February 26-28, 2019*, pages 221–234. USENIX Association, 2019.
- [59] Yibo Zhu, Haggai Eran, Daniel Firestone, Chuanxiong Guo, Marina Lipshteyn, Yehonatan Liron, Jitendra Padhye, Shachar Raindel, Mohamad Haj Yahia, and Ming Zhang. Congestion control for large-scale RDMA deployments. In Steve Uhlig, Olaf Maennel, Brad Karp, and Jitendra Padhye, editors, *Proceedings of the 2015 ACM Conference on Special Interest Group on Data Communication, SIGCOMM 2015, London, United Kingdom, August 17-21, 2015*, pages 523–536. ACM, 2015.
- [60] Danyang Zhuo, Monia Ghobadi, Ratul Mahajan, Klaus-Tycho Förster, Arvind Krishnamurthy, and Thomas E. Anderson. Understanding and mitigating packet corruption in data center networks. In *Proceedings of the Conference of the ACM Special Interest Group on Data Communication, SIGCOMM 2017, Los Angeles, CA, USA, August 21-25, 2017*, pages 362–375. ACM, 2017.

A IMPACT OF PAUSE THRESHOLD

A consequence of the simplicity of BFC's backpressure mechanism is that a flow can temporarily run out of packets at a bottleneck switch while the flow still has packets to send. The pause threshold (Th) governs the frequency of such events. Using a simple model, we quantify the impact of Th .

Consider a long flow f bottlenecked at a switch S . To isolate the impact of the delay in resuming, we assume that f is not sharing a queue with other flows at S or the upstream switch. Let μ_f be the dequeue rate of f at S , i.e., when f has packets in S , the packets are drained at a steady rate of μ_f . Similarly, let $\mu_f \cdot x$ be the enqueue rate of f at the switch, i.e., if f is not paused at the upstream, S receives packets from f at a steady rate of $\mu_f \cdot x$. Here, x denotes the ratio of enqueue to dequeue rate at S . Since f is bottlenecked at S , $x > 1$.

We now derive the fraction of time in steady state that f will not have packets in S . We show that this fraction depends only on x and Th , and is thereby referred as $E_f(x, Th)$.

The queue occupancy for f will be cyclic with three phases.

- Phase 1: S is receiving packets from f and the queue occupancy is increasing.
- Phase 2: S is *not* receiving packets from f and the queue is draining.
- Phase 3: S is not receiving packets from f while the queue is empty.

The time period for phase 1 (t_{p1}) can be calculated as follows. The queue occupancy at start of the phase is 0 and S is receiving packets from f . f gets paused when the queue occupancy exceeds Th . The queue builds at the rate $\mu_f \cdot x - \mu_f$ (enqueue rate - dequeue rate). The pause is triggered after $\frac{Th}{\mu_f \cdot (x-1)}$ time from the start of the phase. Since the pause takes an $HRTT$ to take effect, the queue grows for an additional $HRTT$. t_{p1} is therefore given by:

$$t_{p1} = \frac{Th}{\mu_f \cdot (x-1)} + HRTT. \quad (1)$$

The queue occupancy at the end of phase 1 is $Th + HRTT \cdot \mu_f \cdot (x-1)$. The time period for phase 2 (t_{p2}) corresponds to the time to drain the queue. t_{p2} is given by:

$$t_{p2} = \frac{Th + HRTT \cdot \mu_f \cdot (x-1)}{\mu_f}. \quad (2)$$

At the end of phase 2, there are no packets from f in S . As a result, S resumes f at the upstream. Since the resume takes an $HRTT$ to take effect, the queue is empty for an $HRTT$. Time period for phase 3 (t_{p3}) is given by:

$$t_{p3} = HRTT \quad (3)$$

Combining the equations, $E_f(x, Th)$ is given by:

$$\begin{aligned} E_f(x, Th) &= \frac{t_{p3}}{t_{p1} + t_{p2} + t_{p3}} \\ &= \frac{x-1}{\frac{Th}{HRTT \cdot \mu_f} \cdot x + (x^2 - 1)}. \end{aligned} \quad (4)$$

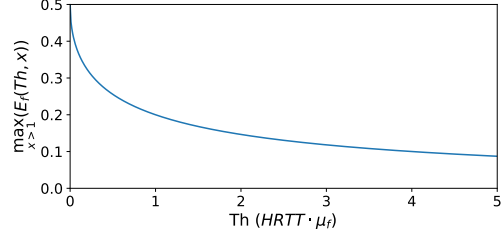


Figure 15: Impact of pause threshold (Th) on the metric of worst case inefficiency. Increasing Th reduces the maximum value for the fraction of time f can run out of packets at the bottleneck.

Notice that for a given x , $E_f(x, Th)$ reduces as we increase Th . Increasing Th , increases the time period for phase 1 and phase 2, and the fraction of time f runs out of packets reduces as a result.

We now quantify the impact of pause threshold on the worst case (maximum) value of $E_f(x, Th)$. Given a Th , $E_f(x, Th)$ varies with x . When $x \rightarrow 1$, $(E_f(x, Th)) \rightarrow 0$, and when $x \rightarrow \infty$, $(E_f(x, Th)) \rightarrow 0$. The maxima occurs somewhere in between. More concretely, for a given value of Th , the maxima occurs at $x = \sqrt{\frac{Th}{HRTT \cdot \mu_f}} + 1$. The maximum value ($\max_{x>1}(E_f(x, Th))$) is given by:

$$\max_{x>1}(E_f(x, Th)) = \frac{1}{\left(\sqrt{\frac{Th}{HRTT \cdot \mu_f}} + 1\right)^2 + 1}. \quad (5)$$

Fig. 15 shows how $\max_{x>1}(E_f(x, Th))$ changes as we increase the pause threshold. As expected, increasing the pause threshold reduces $\max_{x>1}(E_f(x, Th))$. However, increasing the pause threshold has diminishing returns. Additionally, increasing Th increases the buffering for f (linearly).

In BFC, we set Th to 1-Hop BDP at the queue drain rate, i.e., $Th = HRTT \cdot \mu_f$. Therefore, the maximum value of $E_f(x, Th)$ is 0.2 (at $x=2$). This implies, under our assumptions, that a flow runs out of packets at most 20% of the time due to the delay in resuming a flow.

Note that 20% is the maximum value for $E_f(x, Th)$. When $x \neq 2$, $E_f(x, Th)$ is lower. For example, when $x = 1.1$ (i.e., the enqueue rate is 10% higher than the dequeue rate), $E_f(x, Th)$ is only 7.6%.

The above analysis suggests that the worst-case under-utilization caused by delay in resuming is 20%. Note that in practice, when an egress port is congested, there are typically multiple flows concurrently active at that egress. In such scenarios, the under-utilization is much less than this worst-case bound, because it is unlikely that all flows run out of packets at the same time. As our evaluation shows, with BFC, flows achieve close to ideal throughput in realistic traffic scenarios (§6).

B DEADLOCK PREVENTION

We formally prove that BFC is deadlock-free in absence of cyclic buffer dependency. Inspired by Tagger [29], we define a backpressure graph $(G(V, E))$ as follows:

1. Node in the graph (V): A node is an egress port in a switch and can thus be represented by the pair $\langle \text{switchID}, \text{portID} \rangle$.

egressPort>.

- Edge in the graph (E): There is a directed edge from $B \rightarrow A$, if a packet can go from A to B in a single hop (i.e., without traversing any other nodes) and trigger backpressure from $B \rightarrow A$. Edges represent how backpressure can propagate in the topology.

We define deadlock as a situation when a node (egress port) contains a queue that has been paused indefinitely. Cyclic buffer dependency is formally defined as the situation when G contains a cycle.

Theorem 1 *BFC is deadlock-free if $G(V, E)$ does not contain any cycles.*

Proof: We prove the theorem by using contradiction.

Consider a node A that is deadlocked. A must contain a queue (A_q) that has been indefinitely paused as a result of backpressure from the downstream switch. If all the packets sent by A_q were drained from the downstream switch, then A_q will get unpaused (§3.3.2). There must be at least one node (B) in the downstream switch that triggered backpressure to A_q but hasn't been able to drain packets from A_q , i.e., B is deadlocked. This implies, in G , there must be an edge from $B \rightarrow A$. Applying induction, for B there must exist another node C (at the downstream switch of B) that is also deadlocked (again there must be an edge from $C \rightarrow B$). Therefore, there will be an infinite chain of nodes which are paused indefinitely, the nodes of the chain must form a path in G . Since G doesn't have any cycles, the paths in G can only be of finite length, and therefore, the chain cannot be infinitely long. A contradiction, hence proved.

Preventing deadlocks: To prevent deadlocks, given a topology, we calculate the backpressure graph, and pre-compute the edges that should be removed so that the backpressure graph doesn't contain any cycles. Removing these edges thus guarantees that there will be no deadlocks even under link failures or routing errors. To identify the set of edges that should be removed we can leverage existing work [29].

To remove a backpressure edge $B \rightarrow A$, we use the simple strategy of skipping the backpressure operation for packets coming from A going to B at the switch corresponding to B .⁵ Note that, a switch can identify such packets *locally* using the ingress and egress port of the packet. This information can be stored as a match-action-table (indexed by the ingress and egress port) to check whether we should execute the backpressure operations for the packet.

For clos topologies, this just includes backpressure edges corresponding to packets that are coming from a higher layer and going back to a higher layer (this can happen due to rerouting in case of link failures). Note that, usually the fraction of such

⁵To remove backpressure edges in PFC, Tagger uses a more complex approach that involves creating new cycle free backpressure edges corresponding to the backpressure edges that should be removed. To ensure losslessness, Tagger generates backpressure using these new cycle free edges instead of the original backpressure edge. In our proposed solution, we forgo such requirement for simplicity.

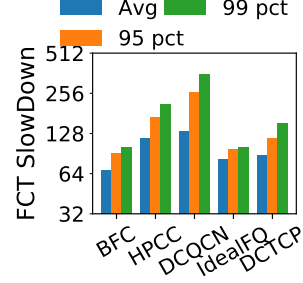


Figure 16: FCT slowdown for incast traffic. Slowdown is defined per flow. For the 100-way incast simulated here, the best case average slowdown is 50, the best case 95th percentile slowdown is 95, and the best case 99th percentile slowdown is 99. BFC reduces the FCT for incast flows compared to other feasible schemes. Setup from Fig. 9.

packets is small ($< 0.002\%$ [29]), so forgoing backpressure for a small fraction of such packets, should hurt performance marginally (if at all).

C INCAST FLOW PERFORMANCE

Fig. 16 shows the slowdown for incast flows for the Google workload used in Fig. 9. Note that the incast flows are 100-way, so the best case average slowdown would be 50 with a shortest-remaining time first scheduling algorithm. Likewise, the best case 99th percentile slowdown is 99. Relative to idealized fair queueing with infinite queues and infinite buffering at each switch, BFC is close to optimal at the tail for incast flows. The benefits of BFC for non-incast traffic do not come at the expense of worse incast performance. Indeed, BFC improves the performance of incast flows relative to end-to-end congestion control, because it reacts faster when capacity becomes available at the bottleneck, reducing the percentage of time the bottleneck is unused while the incast is active.

D USING TCP SLOW-START

We also evaluate the impact of using TCP slow-start instead of starting flows at line rate in Figure 17. We compare the original DCTCP with slow start (DCTCP + SS) with an initial window of 10 packets versus the modified DCTCP used so far (initial window of the BDP). The setup is same as Fig. 12.

With incast, DCTCP + SS reduces buffer occupancy by reducing the intensity of incast flows, improving tail latency (Fig. 17a). However, slow start increases the median FCT substantially (Fig. 17c). Flows start at a lower rate, taking longer to ramp up to the desired rate. For applications with serially dependent flows, an increase in median FCTs can impact the performance substantially.

In the absence of incast, slow start increases both the tail (Fig. 17b) and median (Fig. 17d) FCT for the majority of flow sizes. In particular, short flows are still slower than with BFC, as slow start does not remove burstiness in buffer occupancy in the tail.

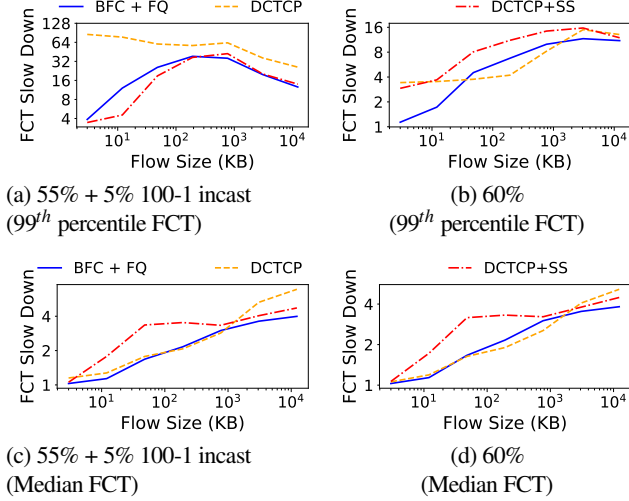


Figure 17: Impact of using slow start on median and 99th percentile tail latency FCT slowdown, for the Facebook flow size distribution with and without incast (setup the same as Fig. 12). With incast, DCTCP + SS (slow start) reduces the tail FCT, but it increases median FCTs by up to $2\times$. In the absence of incast, DCTCP + SS increases both the tail and median FCT for short and medium flows.

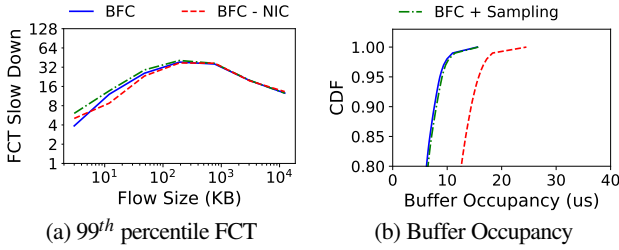


Figure 18: FCT slowdown (99th percentile) and buffer occupancy distribution for two BFC variants. When NICs don't respond to backpressure (BFC - NIC), BFC experiences moderate increased buffering. Using sampling to reduce recirculation (BFC + sampling) has marginal impact on performance.

E ADDITIONAL EXPERIMENTS

E.1 Incremental Deployment

We repeated the experiment in Fig. 11a in the scenario where i) BFC is deployed in part of the network; ii) The switch doesn't have enough capacity to handle all the recirculations. Fig. 18 reports the tail FCT and buffer occupancy for these settings.

Partial deployment in the network: We first evaluate the situation when BFC is only deployed at the switches and the sender NICs don't respond to backpressure signal (shown as BFC - NIC). To prevent sender NIC traffic from filling up the buffers at the ToR, we assume a simple end-to-end congestion control strategy where the sender NIC caps the in-flight packets for a flow to 1 end-to-end bandwidth delay product (BDP). As expected, BFC - NIC experiences increased buffering at the ToR (Fig. 18b). However, the tail buffer occupancy is still below the buffer size and there are no drops. Since all the switches are BFC enabled and following dynamic queue assignment, the frequency of collisions and hence the FCTs are similar to the original BFC.

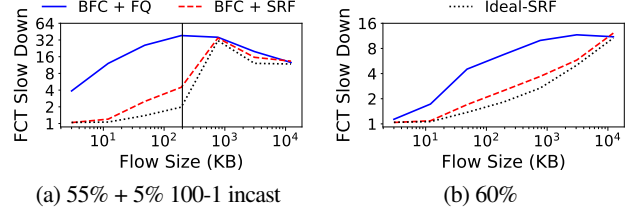


Figure 19: Tail latency FCT slowdown (99th percentile) for different flow sizes as a function of scheduling policy. BFC + SRF (shortest remaining flow first) reduces tail latency FCTs for short and medium sized flows by prioritizing packets from flows that are closest to completion.

Sampling packets to reduce recirculations: A BFC switch with an RMT architecture [15] recirculates packets to execute the dequeue operations at the ingress port. Depending on the packet size distribution of the workload, a switch might not have enough packet processing (pps) capacity or recirculation bandwidth to process these recirculated packets. In such scenarios, we can reduce recirculations by sampling packets. Sampling works as follows.

On a packet arrival (enqueue), sample to decide whether a packet should be recirculated or not. Only increment the pause counter and `size` in the flow table for packets that should be recirculated. The dequeue operations remain as is and are only executed on the recirculated packets. The `size` now counts the packets sampled for recirculation and residing in the switch. While sampling reduces recirculations, it can cause packet reordering. Recall, BFC uses `size` to decide when to reassign a queue. With sampling, `size` can be zero even when a flow has packets in the switch. This means, a flow's queue assignment can change when it already has packets in the switch, causing reordering. However, sticky queue assignment should reduce the frequency of these events (§3.3.2).

We now evaluate the impact of sampling on the performance of BFC (shown as BFC + Sampling). In the experiment, the sampling frequency is set to 50%, i.e., only 50% of the packets are recirculated. BFC + Sampling achieves nearly identical tail latency FCT slowdowns and switch buffer occupancy as the original BFC. With sampling, fewer than 0.04% of the packets were retransmitted due to packet reordering.

E.2 Impact of scheduling policy

The design of BFC is orthogonal to the scheduling policy. We repeated the experiment from Fig. 11, but changed the scheduling policy at the switch from fair queuing (FQ) to shortest remaining flow first (SRF). SRF schedules flows in the order of the amount of data remaining to complete the flow. This has been shown to be optimal for optimizing FCTs [7]. Note that SRF requires end-host knowledge of flow sizes and packet annotation with that information. Fig. 19 shows the 99th percentile FCT slowdowns. We also show Ideal-SRF, an ideal realization of SRF without any restrictions on the number of queues or buffer size. For BFC + SRF and Ideal-SRF, we assume the flow size is known apriori. As expected, BFC + SRF reduces FCTs compared to BFC + FQ (BFC using deficit round robin among active flows), both

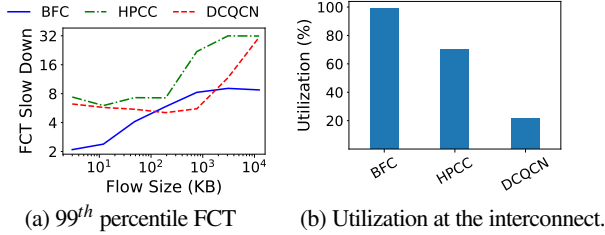


Figure 20: Performance in cross data center environment where two data center are connected by a 200 μ s link, for the Facebook workload (60% load) with no incast traffic. The left figure shows the 99th percentile FCT slowdown for intra-data center flows. The right figure shows the average utilization of the link connecting the two data centers.

with and without incast traffic. BFC + SRF tracks the optimal (Ideal-SRF) closely. With SRF instead of fair queueing, flows finish faster. Thus, the number of active flows queued per egress is smaller, and so BFC + SRF incurs fewer collisions and less HoL blocking than with BFC + FQ.

In the presence of incast, for both BFC + SRF and Ideal-SRF, there is jump in the tail FCT for flows with size bigger than the incast flow size (200 KB, shown as a vertical line in Fig. 19a). This is because SRF schedules the incast flows ahead of these longer flows. Note that while SRF reduces FCTs, it does not ensure fairness and can lead to starvation. Thus, the choice of scheduling policy depends on the requirements of the data center operator.

E.3 Cross data center traffic

For fault tolerance, many data center applications replicate their data to nearby data centers (e.g., to a nearby metro area). We evaluate the impact of BFC on managing cross-data center congestion in such scenarios. We consider the ability of different systems to achieve good throughput for the inter-data center traffic, and we also consider the impact of the cross-data center traffic on tail latency of local traffic, as the larger bandwidth-delay product means more data is in-flight when it arrives at the bottleneck.

We created a Clos topology with 64 leaf servers, and 100 Gbps links and 12 MB switch buffers. Two gateway switches connect the data centers using a 200 Gbps link with 200 μ s of one-way delay (i.e. the base round trip delay of the link is 400 μ s), or roughly equivalent to the two data centers being separated by 50 km assuming a direct connection. The experiment consists of intra-data center flows derived from the Facebook distribution (60% load). Additionally, there are 20 long-lived inter-data center flows in both the directions.

Fig. 20a shows the 99th percentile tail latency in FCT slowdown for intra-data center flows for BFC, HPCC and DCQCN.⁶ Fig. 20b shows the average utilization of the link connecting the two data centers (interconnect), a proxy for the aggregate throughput of the long-lived inter-data center flows. BFC is better for both types of flows. With BFC, the link utilization of the wide area interconnect is close to 100%, while neither HPCC nor DCQCN can maintain the link at full utilization, even with ample

⁶Data center operators have developed specialized protocols for better inter-data center link management [18]; comparing those to BFC is future work.

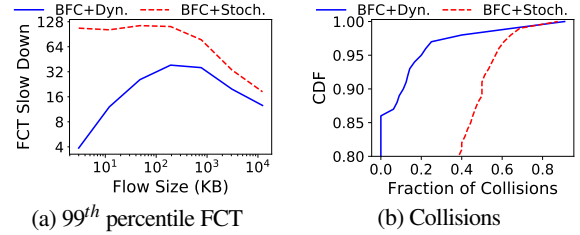


Figure 21: Performance of BFC with stochastic queue assignment, for the workload in Fig. 11a. BFC + Stochastic incurs more queue collisions leading to worse tail latency especially for small flows compared to BFC + Dynamic.

parallelism. This is likely a consequence of slow end-to-end reaction of the inter-data center flows [47]. The congestion state on the links within a data center is changing rapidly because of the shorter intra-data center flows. By the time an inter-data center flow receives congestion feedback and adjusts its rate, the congestion state in the network might have already changed. When capacity becomes available, the inter-data center flows can fail to ramp up quickly enough, hurting its throughput.

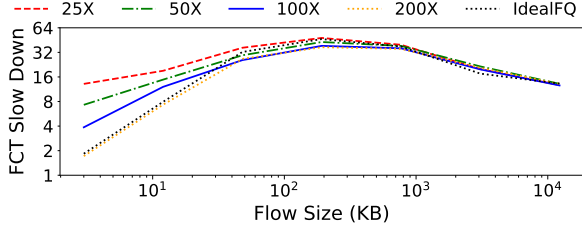
Relative to the single data center case (cf. Fig. 11b), tail latency FCTs are worse for all three protocols, but the relative advantage of BFC is maintained. Where HPCC has better tail latency than DCQCN in the single data center case for both short and medium-sized flows, once inter-data center traffic is added, HPCC becomes worse than DCQCN. With bursty workloads, on the onset of congestion, the long-lived flow will take an end-to-end RTT to reduce its rate, and can build up to 1 BDP (or 500 KB) of buffering, hurting the tail latency of intra-data center traffic. This has less of an impact on DCQCN because it utilizes less of the inter-data center bandwidth in the first place.

In contrast, BFC reacts at the scale of the hop-by-hop RTT. Even though inter-data center flows have higher end-to-end RTTs, on switches within the data center, BFC will pause/resume flows on a hop-by-hop RTT timescale (2 μ s). As a result, with BFC, tail latencies of intra-data center flows are relatively unaffected by the presence of inter-data center flows, while the opposite is true of HPCC.

E.4 Physical queue assignment

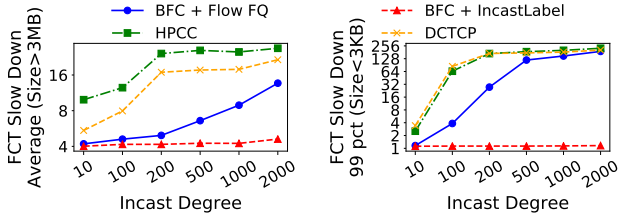
To understand the importance of dynamically assigning flows to physical queues, we repeated the experiment in Fig. 11a with a variant of BFC, BFC + Stochastic, where we use stochastic hashing to statically assign flows to physical queues (as in SFQ). In BFC (referred as BFC + Dynamic here), the physical queue assignment is dynamic. To isolate the effect of changing the physical queue assignment, the pause thresholds are the same as BFC + Dynamic.

Fig. 21a shows the tail latency. Compared to BFC, tail latency for BFC + Stochastic is much worse for all flow sizes. Without the dynamic queue assignment, flows are often hashed to the same physical queue, triggering HoL-blocking and hurting tail latency, even when there are unoccupied physical queues. Fig. 21b is the CDF of such collisions. BFC+Stochastic



(a) 99th percentile FCT

Figure 22: FCT slowdown (99th percentile) for BFC for different size flows as a function of the size of the flow table (as a multiple of the number of queues in the switch). The other experiments in the paper use a flow table of 100X. Further reducing the size of the flow table hurts small flow performance.



(a) Average FCT for long flows

(b) Tail FCT for short flows

Figure 23: FCT slowdown for short and long flows as a function of incast degree. The x axis is not to scale. By isolating incast flows, BFC + IncastLabel reduces collisions and achieves the best performance.

experiences collisions in a high fraction of cases and flows end up being paused unnecessarily. Such flows finish later, further increasing the number of active flows and collisions. Even with incast, the number of active flows in BFC is smaller than the physical queues most of the time.

E.5 Size of flow table

We repeated the experiment in Fig. 11a, but varied the size of the flow table (as a function of the number of queues in the

switch). The default in the rest of the paper uses a flow table of 100X. Fig. 22 shows the tail latency as a function of flow size, for both smaller and larger flow tables. Reducing the size of the flow table increases the index collisions in the flow table. Each flow table collision means that those flows are necessarily assigned to the same physical queue. Tail latency FCTs degrade as a result, particularly for small flows and for smaller table sizes. This experiment shows that increasing the size of the flow table would moderately improve short flow tail latency for BFC.

E.6 Reducing contention for queues

To reduce contention for queues under incast, we tried a variant of BFC where the sender labels incast flows explicitly (similar to [44]). BFC + IncastLabel assigns all the incast flows at an egress port to the same queue. This frees up queues for non-incast traffic, reducing collisions and allowing the scheduler to share the link between incast and non-incast traffic more fairly.

Fig. 23 shows the performance of BFC + IncastLabel in the same setup as Fig. 14. The original BFC is shown as BFC + Flow FQ for per-flow fair queuing. BFC + IncastLabel achieves the best performance across all the scenarios. However, the FCTs for incast flows is higher compared to BFC + Flow FQ (numbers not shown here). When there are multiple incast flows at an ingress port, the incast flows are allocated less bandwidth in aggregate compared to per-flow fair queuing.

While BFC + IncastLabel achieves great performance, it assumes the application is able to label incast flows, and so we use a more conservative design for the main body for our evaluation.